Published online 5 February 2014 *Nucleic Acids Research, 2014, Vol. 42, No. 8* ***5109–5124***
doi:10.1093/nar/gku108

Coexistence of bacterial leucyl-tRNA synthetases with archaeal tRNA binding domains that distinguish $tRNA^{Leu}$ in the archaeal mode

Zhi-Peng Fang, Meng Wang, Zhi-Rong Ruan, Min Tan, Ru-Juan Liu, Mi Zhou, Xiao-Long Zhou* and En-Duo Wang*

Center for RNA Research, State Key Laboratory of Molecular Biology, Institute of Biochemistry and Cell Biology, Shanghai Institutes for Biological Sciences, The Chinese Academy of Sciences, 320 Yue Yang Road, Shanghai 200031, China

Received August 30, 2013; Revised January 10, 2014; Accepted January 13, 2014

ABSTRACT

Leucyl-tRNA (transfer RNA) synthetase (LeuRS) is a multi-domain enzyme, which is divided into bacterial and archaeal/eukaryotic types. In general, one specific LeuRS, the domains of which are of the same type, exists in a single cell compartment. However, some species, such as the haloalkaliphile *Natrialba magadii*, encode two cytoplasmic LeuRSs, *Nm*LeuRS1 and *Nm*LeuRS2, which are the first examples of naturally occurring chimeric enzymes with different domains of bacterial and archaeal types. Furthermore, *N. magadii* encodes typical archaeal $tRNA^{Leu}$s. The tRNA recognition mode, aminoacylation and translational quality control activities of these two LeuRSs are interesting questions to be addressed. Herein, active *Nm*LeuRS1 and *Nm*LeuRS2 were successfully purified after gene expression in *Escherichia coli*. Under the optimized aminoacylation conditions, we discovered that they distinguished cognate *Nm*$tRNA^{Leu}$ in the archaeal mode, whereas the N-terminal region was of the bacterial type. However, *Nm*LeuRS1 exhibited much higher aminoacylation and editing activity than *Nm*LeuRS2, suggesting that *Nm*LeuRS1 is more likely to generate Leu-$tRNA^{Leu}$ for protein biosynthesis. Moreover, using *Nm*LeuRS1 as a model, we demonstrated misactivation of several non-cognate amino acids, and accuracy of protein synthesis was maintained mainly via post-transfer editing. This comprehensive study of the *Nm*LeuRS/$tRNA^{Leu}$ system provides a detailed understanding of the coevolution of aminoacyl-tRNA synthetases and tRNA.

INTRODUCTION

Protein biosynthesis is an essential step in all three domains of life (1). This complicated process requires a subset of proteins and nucleic acids. Aminoacyl-tRNA (transfer RNA) synthetases (aaRSs) are responsible for providing aminoacyl-tRNAs (aa-tRNAs) as the building blocks for protein biosynthesis by catalyzing the esterification of specific amino acids to their cognate tRNAs (2). This reaction (aminoacylation) is performed in two steps by most aaRSs; the amino acid is first activated with adenosine triphosphate (ATP) to form aminoacyl-adenylate (aa-AMP), which is then transferred to the 3′-terminus of the cognate tRNA to generate aa-tRNA for delivery to the ribosomes for protein biosynthesis. The aaRSs are divided into two classes (class I and class II) on the basis of conserved sequences and characteristic structural motifs (3,4). Leucyl-tRNA synthetase (LeuRS) belongs to class I aaRSs, which share a structurally similar Rossmann fold with two characteristic 'HIGH' and 'KMSKS' motifs in the catalytic domain.

Aminoacylation of tRNA requires precise regulation of the velocity of the aa-tRNA production for the ribosome and tight control of aberrant aa-tRNA synthesis (5). Various identity determinants and/or antideterminants are harbored by different tRNAs to facilitate the selection of cognate tRNA from a large set of tRNA species by specific aaRSs. However, the specificity of cognate amino acid activation is greatly challenged by the presence of various non-cognate amino acids and amino acid metabolites, which differ only in the side chain. Taking the mistranslation frequency (1/3000) in protein

*To whom correspondence should be addressed. Tel: +86 21 5492 1241; Fax: +86 21 5492 1011; Email: edwang@sibcb.ac.cn
Correspondence may also be addressed to Xiao-Long Zhou. Tel: +86 21 5492 1242; Fax: +86 21 5492 1011; Email: xlzhou@sibcb.ac.cn

biosynthesis as the threshold (6), a proofreading (editing) mechanism is necessary for half of aaRSs to maintain accuracy during aa-tRNA synthesis. The editing activity can be divided further into the pre- and post-transfer editing. Pre-transfer editing refers to the hydrolysis of the misactivated aa-AMP either in the absence of cognate tRNA (tRNA-independent pre-transfer editing) or in the presence of cognate tRNA (tRNA-dependent pre-transfer editing), whereas post-transfer editing is performed by the editing domain [such as the connective peptide 1 (CP1) domain of class Ia synthetases (7), the N2 domain of class II threonyl-tRNA synthetase (8), the freestanding editing domain homologs (9)] after a misactivated amino acid has been loaded onto the cognate tRNA. The editing activity of an aaRS is of crucial importance in ensuring overall translational quality control. The impairment or loss of editing activity can lead to mistranslation and further ambiguity of the proteome with serious negative influences on the cellular function of most organisms (10–12). This is directly illustrated by the development of neurodegeneration in a mouse model with partial loss of the editing activity of alanyl-tRNA synthetase (13).

LeuRSs catalyze aminoacylation and editing reactions to synthesize Leu-$tRNA^{Leu}$ and to prevent production of mischarged $tRNA^{Leu}$. Based on the primary sequence, relative domain position and orientation, LeuRS can be divided into bacterial (existing in bacteria and organelles) and archaeal/eukaryotic types (existing in eukaryotes and most archaea) (14,15). Both types of LeuRSs contain a Rossmann-fold domain (for amino acid activation and tRNA charging), a CP1 domain (for editing), an α-helix bundle domain (for tRNA binding) and a C-terminal domain (CTD, for tRNA binding) (16). Moreover, LeuRSs also contain some specific insertion domains, such as the leucine-specific domain to modulate their aminoacylation and editing activities (17,18). To date, all the domains identified in a single LeuRS polypeptide are of the same type, indicating that no gene (fragment) rearrangement or fusion between two LeuRS types has occurred.

LeuRSs use different $tRNA^{Leu}$ discrimination modes besides recognition of the common specific discriminator base (A73) of $tRNA^{Leu}$. Biochemical (19,20) and 3D structural (21) data have revealed that the T-loop, D-loop and bases (47f–47i) on one side of the long variable stem in $tRNA^{Leu}$ from bacteria (e.g. *Escherichia coli*) are recognized by the CTD in bacterial *Ec*LeuRS or *Mycobacterium tuberculosis* LeuRS. In the hyperthermophilic bacteria *Aquifex aeolicus*, which contains a heterodimeric LeuRS, the core structure of tRNA formed by the tertiary interactions (U8-A14, G18-U55 and G19-C56) and the orientation of the long variable stem are critical elements for $tRNA^{Leu}$ aminoacylation, and the anticodon stem acts as an additional determinant for editing by LeuRS (22). In *Homo sapiens*, three base pairs (C3:G70, A4:U69 and G5:C68) in the acceptor stem, C20a in the D-loop, the length of long variable stem and the number of the unpaired residues in long variable loop are the identity elements of $tRNA^{Leu}$ (23). However, *Saccharomyces cerevisiae* uses the anticodon loop of $tRNA^{Leu}$ (A35 and G37) as the major identity determinant (24). The recognition mode of $tRNA^{Leu}$ in archaea is highly conserved and differs from those of the previously mentioned species. The most obvious feature is the critical dependence on the two absolutely conserved bases (A47c, G47d) at the tip of the long variable loop in $tRNA^{Leu}$, as reported in halophilic *Haloferax volcanii* and thermophilic *Pyrococcus horikoshii* (25,26). The 3D structure of the *P. horikoshii* LeuRS (*Ph*LeuRS) showed that its CTD, which contains five α-helices, antiparallel β-sheets and many flexible loops, is responsible for tRNA recognition, especially of Asp845, Ile849 and the last few conserved residues (Pro962, Ile964, Ile966 and Glu967) (26). Deletion of more than one residue in the CTD led to the total loss of aminoacylation activity of *Ph*LeuRS. In contrast, deletion of the entire CTD had no effect on its editing activity (14).

The distribution of LeuRSs is diverse in the three domains of life. In bacteria (e.g. *E. coli*), only a bacterial LeuRS is encoded. Eukaryotes (e.g. *H. sapiens*) generally contain two LeuRSs: an archaeal/eukaryotic cytoplasmic form and a bacterial form in mitochondria and/or chloroplasts. A majority of archaeal (e.g. *P. horikoshii*) encode a LeuRS, which is evolutionarily close to the cytoplasmic form of the enzyme in eukaryotes. However, in a limited number of cases, such as the halobacteria *Natrialba magadii*, which thrives in alkaline and hypersaline conditions (pH 9.5, 3.5 M NaCl) (2 g/l KCl, 0.1 g/l $MgSO_4 \cdot 7H_2O$ and microscale of $FeSO_4$ and $MnCl_2$ are also needed in the culture medium) (27,28), the LeuRS/$tRNA^{Leu}$ system exhibits several striking features. First, the *N. magadii* genome encodes two LeuRS genes [designated as *Nm*LeuRS1 (accession No. YP_003479843.1, 904-aa) and *Nm*LeuRS2 (accession No. YP_003481407.1, 971-aa)] displaying 46% identity. Second, these two LeuRSs exhibit both bacterial and archaeal characteristics. Specifically, the N-terminal region (including the Rossmann fold, the CP1 domain, the CP2 domain and the α-helix bundle domain) shares high homology with bacterial LeuRSs (Supplementary Figure S1A); however, the CTD is highly homologous to its archaeal LeuRS counterpart (Supplementary Figure S1B). Moreover, *N. magadii* expresses typical archaeal $tRNA^{Leu}$s in which the A47c and G47d bases in the long variable loop are absolutely conserved, whereas no bacterial $tRNA^{Leu}$s are expressed (Supplementary Figure S2). This raises the interesting questions of the mechanisms underlying the aminoacylation and editing activities, the active sites of which reside in the bacterial and archaeal portion of two *Nm*LeuRSs as well as the recognition mode for archaeal $tRNA^{Leu}$.

In the present study, genes encoding *Nm*LeuRS1 and *Nm*LeuRS2 were cloned and overexpressed in *E. coli*. Following successful purification, the aminoacylation, amino acid activation, tRNA recognition mode and editing activity of these *Nm*LeuRSs were characterized. Our results provide an improved understanding of the activity and evolutionary pathway of tRNA synthetases from halobacteria.

MATERIALS AND METHODS

Materials

L-leucine (Leu), L-norvaline (Nva), α-amino butyric acid (ABA), L-isoleucine (Ile), L-methionine (Met), tetrasodium pyrophosphate, Tris–HCl, $MgCl_2$, NaCl, KCl and activated charcoal were purchased from Sigma (St Louis, MO, USA). [^{3}H]Leu, [^{32}P]tetrasodium pyrophosphate and [α-^{32}P]ATP were obtained from PerkinElmer (Waltham, MA, USA). Nucleoside triphophate (NTP) and deoxynucleoside triphosphate (dNTP) mixtures were purchased from Sangon Biotech (China). The Pfu DNA polymerase, the DNA fragment rapid purification kit and plasmid extraction kit were purchased from Tiangen Biotech (China). The KOD-plus mutagenesis kit was obtained from TOYOBO (Japan). T4 ligase, inorganic pyrophosphatase, protein ladder (#26614) and restriction endonucleases were obtained from Thermo Scientific (Waltham, MA, USA). The Ni^{2+}-NTA (Ni^{2+}-nitrilotriacetate) Superflow was purchased from Qiagen (Germany). Polyethyleneimine cellulose plates, Amicon Ultra-15 filter and nitrocellulose membranes (0.22 μm) were purchased from Merck (Germany). Oligonucleotide primers were synthesized by Life Technologies (Carlsbad, CA, USA). Competent *E. coli* BL21 (DE3) and Top10 cells were prepared in our laboratory. T7 RNA polymerase (29) and *E. coli* CCA-adding enzyme (30) were purified from an overproduction strain in our laboratory.

Sequence alignment of LeuRSs

For phylogenetic analysis of LeuRSs covering three domains, 63 protein sequences of various LeuRSs from representative species were obtained from the NCBI database (http://www.ncbi.nlm.nih.gov/protein/). Specific sequence alignments were carried out using the Clustal X2 program (31) and subsequent phylogenetic trees were constructed with the MEGA 5.2 program (32) using the minimal evolution algorithm. Bootstrap analysis was performed with 1000 replicates.

Gene cloning and protein purification

*Nm*LeuRS1 and *Nm*LeuRS2 genes were amplified from *N. magadii* ATCC 43099 genomic DNA and cloned into pET28a (pre-cleaved with *Nde*I/*Bam*HI) to produce pET28a-*Nm*LeuRS1 and pET28a-*Nm*LeuRS2. The primers for gene amplification were as follows: *Nm*LeuRS1 forward (5′ ccatatggaaagttatacag3′), *Nm*LeuRS1 reverse (5′ cggatcctcagtcctcgatc3′), *Nm*LeuRS2 forward (5′ ccatatgacaaaccagtacgatc3′) and *Nm*LeuRS2 reverse (5′ cggatcctcactgaatccgaat3′). *Haloarcula hispanica* LeuRS1 and LeuRS2 genes were amplified from *H. hispanica* ATCC 33960 genomic DNA and cloned into pET28a (pre-cleaved with *Nde*I/*Bam*HI or *Nhe*I/*Bam*HI) to produce pET28a-*Hh*LeuRS1 and pET28a-*Hh*LeuRS2. The primers for gene amplification were as follows: *Hh*LeuRS1 forward (5′ ccatatgaccacga ccggtg3′), *Hh*LeuRS1 reverse (5′ cggatccctactcgtcgatgt3′), *Hh*LeuRS2 forward (5′ agctagcatgtcgcgccgatat3′) and *Hh*LeuRS2 reverse (5′ tggatcctcaggagatgtgga3′). *Escherichia coli* BL21 (DE3) cells were transformed with these constructs. A single transformant was selected and cultured in 1 l of 2× Yeast extract and Tryptone (YT) medium (1% yeast extract, 1.6% tryptone and 0.5% NaCl) at 37°C. Cells were cultured to mid-log phase (OD_{600}, 0.6) and protein expression was induced by the addition of isopropyl-1-thio-β-D-galactopyranoside (final concentration, 200 μM). Cells were cultured at 22°C for a further 7 h before centrifugation at 3000*g* for 10 min at 4°C followed by washing with water. Purification was performed by Ni^{2+}-NTA Superflow (Qiagen) chromatography according to the manufacturer's protocol. The wet cells (~3.5 g) were lysed by ultrasonication on ice in 15 ml of buffer A [20 mM, pH 9.0, Tris–HCl, 1.2 M NaCl, 2 mM imidazole, 10% glycerol and 10 mM phenylmethanesulfonyl fluoride]. The lysates were centrifuged at 40 000*g* for 60 min to remove the debris and insoluble fractions. The supernatant was applied to 2 ml of Ni^{2+}-NTA resin mixed gently for 30 min at 4°C and then washed with 20 ml of buffer A and 20 ml of buffer B (20 mM, pH 9.0, Tris–HCl, 1.2 M NaCl, 25 mM imidazole and 10% glycerol) to remove nonspecific binding proteins. Binding proteins were eluted in 10 ml of buffer C (20 mM, pH 9.0, Tris–HCl, 1.2 M NaCl, 250 mM imidazole and 10% glycerol), and the eluted fractions were concentrated and dialyzed with buffer D (20 mM, pH 8.5, Tris–HCl, 3 M KCl, 0.1 M $MgAc_2$ and 5 mM β-mercaptoethanol) (33) using Amicon Ultra-15 filters (Millipore; cutoff 30 kDa). The resulting protein solution was concentrated to ~300 μl, mixed with glycerol to a final concentration of 40% (v/v) and stored at −20°C. Protein concentration was determined by active site titration (34).

Preparation of tRNA^{Leu} transcript and [^{32}P] labeling at 3′ terminus of tRNA

The DNA sequence of the T7 promoter and the *Nm*tRNA^{Leu}(GAG) gene was obtained by ligating three chemically synthetized DNA fragments for each strand, which were then ligated into pTrc99b plasmid (pre-cleaved with *Eco*RI/*Pst*I) to construct pTrc99b-T7-*Nm* tRNA^{Leu}(GAG). The forward primer (5′ ctaatacgact cactatagcgt 3′) and reverse primer (5′ tggtgcgtgggaccggattc 3′) were used to amplify the template for *in vitro* transcription by Pfu polymerase (T7 promoter underlined). The PCR product was extracted by phenol/chloroform and precipitated in three volumes of ethanol and 0.3 M Sodium acetate (NaAc), pH 5.2. The *in vitro* transcription of *Nm*tRNA^{Leu}(GAG) was carried out in a reaction mixture containing 40 mM Tris–HCl, pH 8.0, 22 mM $MgCl_2$, 1 mM spermidine, 5 mM dithiothreitol (DTT), 0.5% Triton X-100, 60 ng/μl tDNA template, 5 mM NTP (each), 1 U/μl ribonuclease inhibitor, 20 mM GMP, 500 U/μl T7 RNA polymerase and 1 U/ml pyrophosphatase for 3 h. Subsequently, 5 U/ml DNase I was added to digest the tDNA template for 1 h. The transcript was separated by 8 M urea −15% PAGE gel electrophoresis. The tRNA was excised from the gel, eluted with 0.5 M NaAc, pH 5.2, at room temperature three times, precipitated with three volumes of ethanol at −20°C and dissolved in 5 mM $MgCl_2$ after centrifugation (15 000*g*, 30 min, 4°C) and drying. The tRNA was

annealed at 85°C for 10 min and cooled naturally in the bath of 1 l water to room temperature for correct folding. *Nm*tRNA^{Leu}(CAA), *Ph*tRNA^{Leu}(GAG) and the corresponding mutants were prepared in the same way.

*Nm*tRNA^{Leu}(GAG) was labeled with [α-^{32}P]ATP as reported previously (35). In detail, 750 pmol tRNA was added in a 50 µl of reaction mixture containing 60 mM Tris–HCl, pH 8.0, 12 mM $MgCl_2$, 1 mM DTT, 50 µM Na_4PPi, 15 µM ATP, 0.666 µM [α-^{32}P]ATP and 10 µM *E. coli* CCA-adding enzyme at 37°C for 5 min. Subsequently, 0.1 U pyrophosphatase was added for a further 5 min. The solution was extracted twice using phenol/chloroform and then precipitated in three volumes of ethanol. The ratio of [^{32}P]-labeled tRNA was determined by liquid scintillation counting of the sample washed with and without 5% trichloroacetic acid.

Aminoacylation, misacylation and deacylation

The aminoacylation assays of *Nm*LeuRSs were carried out in a reaction mixture containing 20 mM Tris–HCl, pH 9.0, 3.5 M KCl, 30 mM $MgCl_2$, 1 mM DTT, 4 mM ATP, 20 µM [^{3}H]Leu (11 Ci/mM), various tRNAs and *Nm*LeuRS1 (50–500 nM) or *Nm*LeuRS2 (2 µM) unless otherwise stated at 40°C. Misacylation was performed under similar conditions with 8.80 µM *Nm*tRNA^{Leu} containing 3.67 nM [^{32}P]*Nm*tRNA^{Leu}, 50 mM Nva or 170 mM ABA or 100 mM Ile or 100 mM Met, and 2 µM *Nm*LeuRSs or their mutants. The misacylated Nva-[^{32}P]*Nm*tRNA^{Leu} was obtained by using *Ph*LeuRS1-D332A. Deacylation of Nva-[^{32}P]*Nm*tRNA^{Leu} was carried out under similar conditions except pH 7.5 with 500 nM *Nm*LeuRSs or mutants were used.

To determine the aminoacylation level of [^{32}P]*Nm*tRNA^{Leu}, the misacylation and deacylation samples were ethanol precipitated, digested by nuclease S1 and then thin-layer chromatography (TLC) was performed to separate Nva-[^{32}P] adenosine monophosphate (AMP) (from Nva-[^{32}P]*Nm*tRNA^{Leu}), [^{32}P]AMP (from [^{32}P]*Nm*tRNA^{Leu}) and [^{32}P]ATP in 0.1 M NH_4Ac and 5% acetic acid. The plates were visualized by autoradiography, and the data were analyzed using MultiGauge Version 3.0 software (FUJIFILM).

Measurement of equilibrium dissociation constants for tRNA by filter binding assays

Nitrocellulose filter binding assays were performed to detect the formation of *Nm*LeuRSs/[^{32}P]-*Nm* tRNA^{Leu}(GAG) complexes at 4°C in a 50 µl of reaction mixture containing 20 mM Tris–HCl, pH 9.0, 3 M KCl, 30 mM $MgCl_2$, 1 mM DTT, 75 nM *Nm*tRNA^{Leu}(GAG) [~13 000 counts per minute (CPM)/pmol, 1 nM [^{32}P]*Nm*tRNA^{Leu}(GAG)] and *Nm*LeuRSs (1–15 µM) for 30 min (36). The mixtures were then filtered through the nitrocellulose membrane (0.22 µm) [preequilibrated in washing buffer (50 mM potassium phosphate, pH 5.5, 50 mM $MgCl_2$) for at least 10 min] and washed twice with 0.3 ml of washing buffer. The membranes then dried before quantitation by radioactivity. Data were analyzed using GraphPad Prism 5 software.

ATP-PPi exchange and AMP formation

ATP-PPi exchange assays were performed at 40°C in a reaction mixture containing 20 mM Tris–HCl, pH 9.0, 3.5 M KCl, 30 mM $MgCl_2$, 1 mM DTT, 4 mM ATP, 2 mM [^{32}P]tetrasodium pyrophosphate, Leu (0.5 µM–10 mM) or Nva (0.05–50 mM) or ABA (0.5–170 mM) and 1 µM *Nm*LeuRS1 or 3 µM *Nm*LeuRS2. Samples at specific time-points were added to 200 µl of quenching solution containing 2% activated charcoal, 3.5% $HClO_4$ and 50 mM tetrasodium pyrophosphate.

AMP formation assays were carried out at 40°C in a reaction mixture containing 20 mM Tris–HCl, pH 9.0, 3.4 M KCl, 30 mM $MgCl_2$, 1 mM DTT, 15 mM Nva, 4 mM [α-^{32}P]ATP, 2 µM *Nm*LeuRS1 or *Nm*Leu RS1-D354A mutant, in the presence or absence of 25 µM *Nm*tRNA^{Leu}(GAG). Samples were quenched in 200 mM NaAc (pH 5.2) and then spotted onto polyethyleneimine cellulose plates. TLC was performed as described previously.

RESULTS

Natrialba magadii encodes two chimeric LeuRSs and archaeal tRNA^{Leu}s

The expanded genome analysis of various species from all three domains of life significantly facilitated gene function investigations. Analysis of LeuRSs from bacteria, archaea and eukaryotes revealed that some halobacteria, such as *N. magadii*, *H. hispanica*, *Halorhabdus utahensis*, *Haloarcula marismortui*, *Halomicrobium mukohataei*, *Haloterrigena turkmenica* and *Haladaptatus paucihalophilus*, and some sulfolobus (e.g. *Sulfolobus islandicus*) harbor two copies of *leuS*, encoding LeuRS. Sequence alignment showed that the N-terminal region of both *Nm*LeuRSs (Met1-Pro756 of *Nm*LeuRS1 and Met1-Pro788 of *Nm*LeuRS2) displayed a high level of homology with the corresponding region of bacterial LeuRSs (e.g. Met1-Pro788 of *Ec*LeuRS) (Supplementary Figure S1A), whereas the CTDs of both *Nm*LeuRSs (Thr757-Asp904 of *Nm*LeuRS1 and Ala789-Gln971 of *Nm*LeuRS2) were highly homologous to their archaeal LeuRS counterparts (e.g. Glu822-Glu967 of *Ph*LeuRS) (Supplementary Figure S1B). This observation was further supported by phylogenetic analysis of either the N-terminal regions or CTDs of LeuRSs from the three domains of life (Figure 1). In particular, the homology or identity of two LeuRSs in a single species was not high. For instance, the protein products *Nm*LeuRS1 and *Nm*LeuRS2 displayed 46.6% identity and 56.9% homology. Consistently, *Nm*LeuRS1 and *Nm*LeuRS2 were in separate branches of the phylogenetic tree, indicating the possibility of horizontal gene transfer, or gene duplication and subsequent divergence.

On the other hand, the *N. magadii* genome has five tRNA^{Leu} genes, including tRNA^{Leu}(GAG), tRNA^{Leu}(CAG), tRNA^{Leu}(UAG), tRNA^{Leu}(CAA) and tRNA^{Leu}(UAA) (37). Sequence analysis of tRNA^{Leu}s revealed that these tRNAs were all archaeal type, with absolutely conserved A47c and G47d bases in the

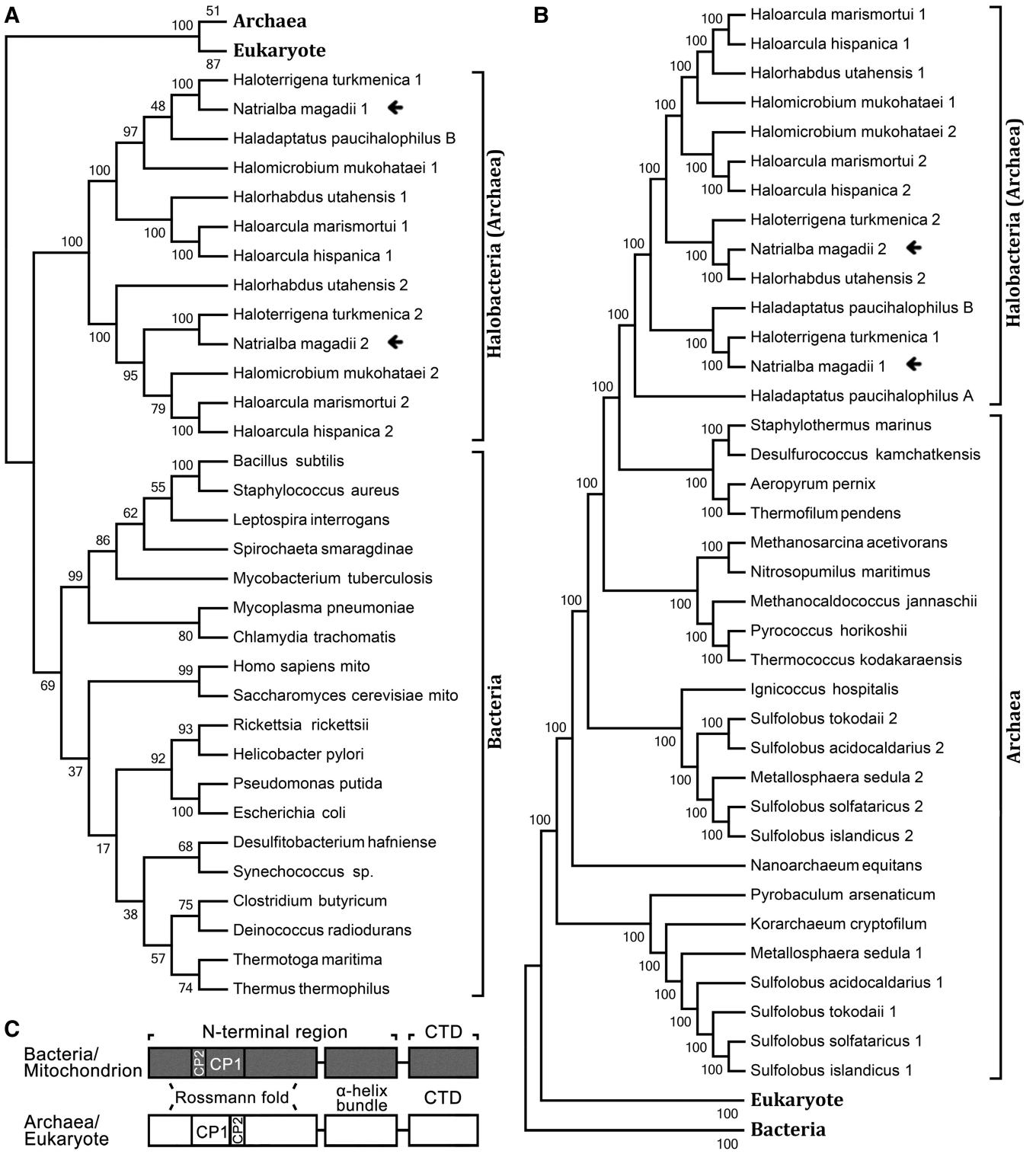

Figure 1. Phylogenetic analyses of LeuRSs from different species. (**A**) Phylogenetic analyses of the N-terminal regions (including Rossmann-fold, CP1, CP2 and α-helix bundle domains) of various LeuRSs. (**B**) Phylogenetic analyses of the C-terminal domains (CTDs) of various LeuRSs. (**C**) Domain scheme of LeuRSs from bacteria/mitochondrion and archaea/eukaryote, respectively. N-terminal regions included Rossmann-fold, CP1, CP2 and α-helix bundle domains.

long variable loop (Supplementary Figure S2). Above all, in halophiles such as *N. magadii*, two LeuRSs and $tRNA^{Leu}$ exhibit chimeric and archaeal features, respectively (Figure 2). To our knowledge, this is the first description of a naturally occurring chimeric LeuRS.

*Nm*LeuRS activity requires high KCl and high pH

To characterize the function of both *Nm*LeuRSs, the genes encoding two *Nm*LeuRSs were overexpressed in *E. coli*. Both *N*mLeuRSs were purified in Tris–HCl buffer, pH 9.0, by Ni^{2+}-NTA affinity chromatography (see 'Materials and Methods' section). In accordance with previous reports (38,39), *Nm*LeuRS1 (102.2 kDa) and *Nm*LeuRS2 (107.6 kDa) migrated slowly in 8% SDS-PAGE gel (Figure 3A) because of the presence of more negative charges with more acidic (Asp, Glu) and less basic (Lys, Arg) amino acid residues in halophilic proteins compared with their mesophilic homologs.

To investigate the aminoacylation reaction, *Nm*LeuRS1 was used initially to determine an appropriate reaction system, followed by investigation of *Nm*LeuRS2. As a halophilic protein, *Nm*LeuRS1 showed a linear increase in aminoacylation activity with increasing KCl concentration above the threshold of 2.5 M. It displayed the highest activity in the presence of 3.75 M KCl (higher KCl concentrations were not evaluated) (Figure 3B). To facilitate preparation of the reaction system, 3.5 M KCl was chosen for use in further assays. Surprisingly, no activity of *Nm*LeuRS1 was detected in NaCl solutions, even at concentrations as high as 4 M (Figure 3B). A similar phenomenon was reported for *H. volcanii* DNA ligase, in that K^+ mediated stabilization and modulation of the enzyme activity, whereas Na^+ did not (40). In contrast, the activity of mesophilic homologs such as *Ec*LeuRS and *Ph*LeuRS was obviously different from that of *Nm*LeuRS1. Although the relative activity of *Ec*LeuRS increased from 20 to 100% after the addition of 0.1 M KCl, that lost in the presence of >0.8 M KCl (Figure 3B). The activity of *Ph*LeuRS was totally inversely correlated with the concentration of KCl, in >0.8 M KCl solution *Ph*LeuRS had no activity (Figure 3B). Similar to

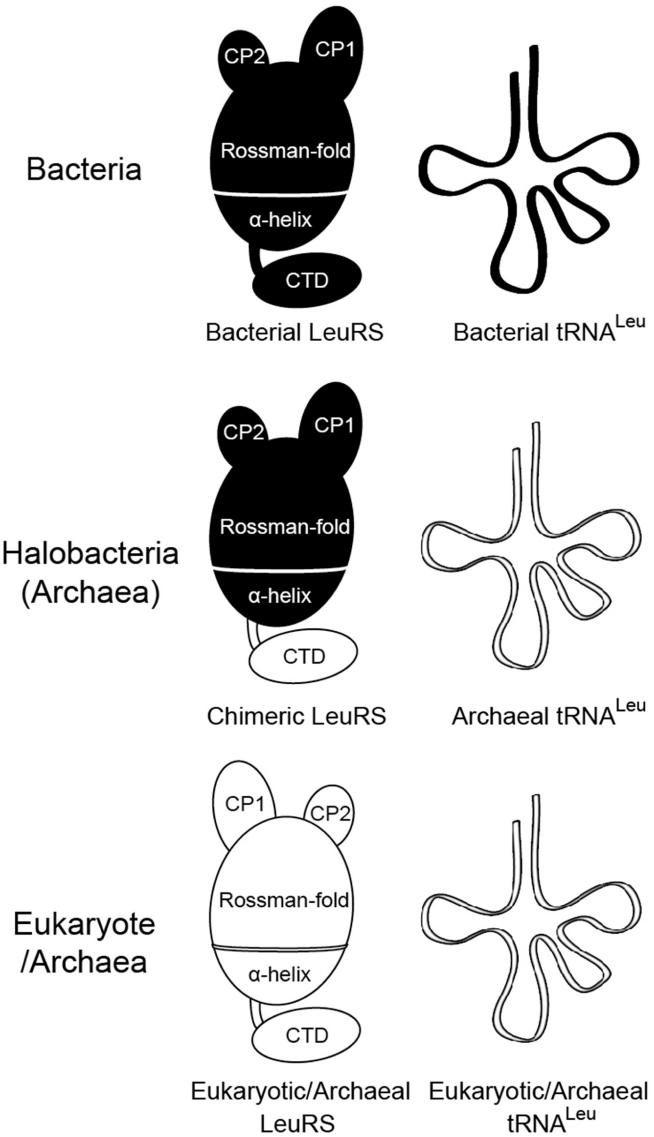

Figure 2. Schema showing the different interaction modes of LeuRS/$tRNA^{Leu}$ in bacteria, halobacteria (archaea) and eukaryote/archaea. The models of LeuRS and $tRNA^{Leu}$ in black and white represent bacterial and archaeal/eukaryotic types, respectively. CP, connective peptide domains; CTD, C-terminal domain.

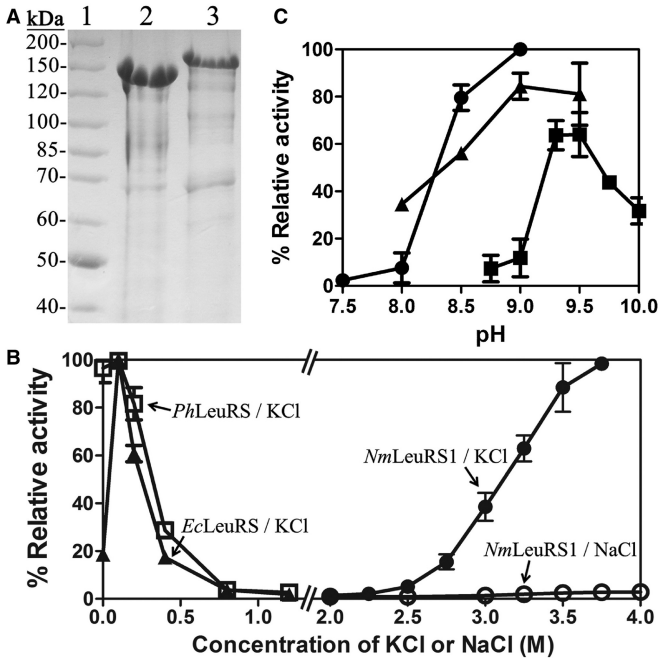

Figure 3. Purification of *Nm*LeuRSs and optimization of aminoacylation conditions. (**A**) A total of 8% SDS-PAGE analysis of the purified *Nm*LeuRSs from *E. coli*. Lanes: 1, 2 and 3 are molecular markers (Thermo Scientific, #26614), *Nm*LeuRS1 and *Nm*LeuRS2, respectively. (**B**) Relative aminoacylation activity of *Nm*LeuRS1, *Ec*LeuRS and *Ph*LeuRS under different KCl or NaCl concentrations. The activities of *Ec*LeuRS in 0.1 M KCl, *Ph*LeuRS in 0 M KCl and *Nm*LeuRS1 in 3.75 M KCl were defined as 100%. (**C**) Relative aminoacylation activities of *Nm*LeuRS1 under different pH conditions in Tris–HCl (black circle), Bis-Tris-propane-HCl (black up-pointing triangle) and CHES-KOH (black square). The activity of *Nm*LeuRS1 in Tris–HCl, pH 9.0, was defined as 100%.

*Nm*LeuRS1, the activity of *Nm*LeuRS2 increased significantly from 2.0–3.1 M KCl; no obvious further stimulation of activity occurred at higher KCl concentrations (Supplementary Figure S3A).

The pH optimization for the amino acylation activities of *Nm*LeuRS1 was then studied. *Nm*LeuRS1 exhibited the highest activity at pH 9.0 in Tris–HCl or Bis-Tris-propane-HCl buffer or at pH 9.5 in CHES-KOH buffer (Figure 3C). The activity decreased obviously at pH 8.0 or below. Similar results were obtained with *Nm*LeuRS2 (Supplementary Figure S3B). High pH is optimal for the activity of many extracellular proteins of alkaliphiles (41,42). However, an almost neutral cytoplasmic pH is maintained by Na^+/H^+ antiporters (43,44) or cell wall macromolecules, which serve as a specific barrier to the flux of relevant ions (45). Our results suggest that the cytoplasmic proteins in *N. magadii* perform their physiological function in an alkaline solution through another mechanism. The genes necessary for survival in alkaline conditions have not been identified in the genome of *N. magadii* (46). The *in vitro* characteristics of recombinant *Nm*LeuRSs may differ in the *in vivo* situation.

Distinct aminoacylation activities of the *Nm*LeuRSs

*Nm*LeuRSs have similar domain architecture, display 46% identity and coexist in a single cell compartment. It is possible that either one or both *Nm*LeuRSs play an essential aminoacylation role in protein biosynthesis. The activities of the two *Nm*LeuRSs were initially compared in ATP-PPi exchange assays. *Nm*LeuRS1 displayed a much higher amino acid activation activity than *Nm*LeuRS2, the K_m value of *Nm*LeuRS2 was nearly 105-fold greater than that of *Nm*LeuRS1 (K_m: 891 ± 2 μM versus 8.43 ± 1.30 μM), and the activation rate of *Nm*LeuRS1 was 58-fold greater than that of *Nm*LeuRS2 [k_{cat}: $(5.63 \pm 0.12) \times 10^{-1}\,s^{-1}$ versus $(9.61 \pm 0.47) \times 10^{-3}\,s^{-1}$] (Table 1).

The aminoacylation assays showed that both *Nm*LeuRSs were able to charge *Nm*tRNA^{Leu}(GAG), *Nm*tRNA^{Leu}(CAA) and *Ph*tRNA^{Leu}(GAG) (the Leu accepting activity of the aforementioned tRNA^{Leu} transcripts was 1350, 1468 and 1225 pmol/A_{260}), although the catalytic efficiencies (k_{cat}/K_m) of *Nm*LeuRS2 for different tRNA^{Leu}s were only 1/130 to 1/40 of those of *Nm*LeuRS1 (Table 2). The data showed a distinct difference in the catalytic velocity (k_{cat}) but not the K_m value for tRNA^{Leu} during aminoacylation, which may be due to the much lower amino acid activation activity of *Nm*LeuRS2. To further define the affinity between *Nm*LeuRSs and *Nm*tRNA^{Leu}(GAG), filter binding assays were performed as reported previously (36). The equilibrium dissociation constants (k_d) of *Nm*LeuRS1 and *Nm*LeuRS2 for *Nm*tRNA^{Leu}(GAG) were 6.36 ± 1.17 μM and 3.36 ± 0.89 μM, respectively (Table 3). These results showed that *Nm*LeuRS2 had obviously decreased aminoacylation activity compared with *Nm*LeuRS1, whereas the affinity for cognate *Nm*tRNA^{Leu} was retained.

Table 1. Leucine activation kinetics constants of *Nm*LeuRSs at 40°C[a]

	K_m (μM)	k_{cat} (s^{-1})	k_{cat}/K_m ($mM^{-1}s^{-1}$)	Activity ratio
*Nm*LeuRS1	8.43 ± 1.30	$(5.63 \pm 0.12) \times 10^{-1}$	66.8	1[b]
*Nm*LeuRS2	891 ± 2	$(9.61 \pm 0.47) \times 10^{-3}$	0.0108	1/6185

[a]The results are the average of three independent repeats with standard deviations indicated.
[b]The activity of *Nm*LeuRS1 for Leu is defined as 1.

*Nm*LeuRS1 showed the highest catalytic activity for *Nm*tRNA^{Leu}(GAG), which was used predominantly (4.93%) among all *Nm*tRNA^{Leu} isoacceptors. The catalytic activity for *Nm*tRNA^{Leu}(CAA) was only half of that for *Nm*tRNA^{Leu}(GAG). In addition, the catalytic activity for the heterologous *Ph*tRNA^{Leu}(GAG) was slightly lower than that for the homologous *Nm*tRNA^{Leu} (Table 2), implying that *Nm*LeuRSs, despite the presence of the bacterial aminoacylation and editing domains, effectively distinguished archaeal tRNA^{Leu}.

To further explore the aminoacylation activities of other coexisted LeuRSs present in halobacteria, we then purified the protein of two *leuS* genes of *H. hispanica* after being overexpressed in *E. coli* [designated as *Hh*LeuRS1 (accession No. YP_004794828.1, 895-aa) and *Hh*LeuRS2 (accession No. YP_004797622.1, 893-aa)] (Supplementary Figure S4A) (47). Similar results with *Nm*LeuRSs were obtained, that *Hh*LeuRS2 had only little amino acid activation and aminoacylation activities, whereas *Hh*LeuRS1 retained the normal activities (Supplementary Figure S4B and C). These results suggested that the coexistence of an active LeuRS and an inactive one might be a widespread phenomenon in halobacteria.

*Nm*LeuRSs distinguish *Nm*tRNA^{Leu} in the archaeal mode

With both bacterial N-terminal regions and an archaeal C-terminal tRNA binding domain, the mechanism by which *Nm*LeuRSs distinguish *Nm*tRNA^{Leu} presents an interesting question. *Nm*LeuRS1 was chosen as a model for this investigation because it exhibited higher activity than *Nm*LeuRS2. Previous investigation of the archaeal *Ph*LeuRS/tRNA^{Leu} system showed that A47c and G47d in the long variable loop of *Ph*tRNA^{Leu} are critical elements, which are recognized by Asp845, Ile849 and the last few conserved residues (Pro962, Ile964, Ile966 and Glu967) of *Ph*LeuRS (26).

We first studied the recognition mode based on analysis of LeuRS. Owing to the high homology between the CTDs of *Nm*LeuRS1 and *Ph*LeuRS, we prepared several deletion mutants at the C-terminus of *Nm*LeuRS1, including *Nm*LeuRS1-ΔE (Glu903 deletion), *Nm*LeuRS1-ΔED (Glu903 and Asp904 deletions), *Nm*LeuRS1-ΔI (Ile902 deletion) and *Nm*LeuRS1-ΔIED (Ile902, Glu903 and Asp904 deletions) (Figure 4A). *Nm*LeuRS1-ΔE showed similar activity compared with the wild-type enzyme, whereas *Nm*LeuRS1-ΔED exhibited an ~60% loss, and *Nm*LeuRS1-ΔIED and *Nm*LeuRS1-ΔI lost their activity completely (Figure 4B), implicating the conserved Ile902 of *Nm*LeuRS1 as the most important residue in recognition. These data suggested that the mode of *Nm*tRNA^{Leu}s distinguished

Table 2. Aminoacylation kinetics of *Nm*LeuRSs at 40°C[a]

$tRNA^{Leu}$	LeuRS	K_m (μM)	k_{cat} (s^{-1})	k_{cat}/K_m ($mM^{-1}s^{-1}$)	Activity ratio
Nm$tRNA^{Leu}$(GAG)	*Nm*LeuRS1	7.73 ± 0.22	$(6.40 \pm 0.19) \times 10^{-2}$	8.28	1[b]
	*Nm*LeuRS2	3.35 ± 0.21	$(6.68 \pm 0.22) \times 10^{-4}$	0.199	1/42
Nm$tRNA^{Leu}$(CAA)	*Nm*LeuRS1	11.01 ± 1.36	$(4.64 \pm 0.34) \times 10^{-2}$	4.21	1/2
	*Nm*LeuRS2	13.13 ± 1.57	$(4.18 \pm 0.50) \times 10^{-4}$	0.0318	1/260
Ph$tRNA^{Leu}$(GAG)	*Nm*LeuRS1	12.51 ± 2.16	$(4.18 \pm 0.60) \times 10^{-2}$	3.34	1/2.5
	*Nm*LeuRS2	16.43 ± 0.62	$(1.19 \pm 0.08) \times 10^{-3}$	0.0724	1/114

[a]The results are the average of three independent repeats with standard deviations indicated.
[b]The activity of *Nm*LeuRS1 for *Nm*$tRNA^{Leu}$(GAG) is defined as 1.

Table 3. k_d of *Nm*$tRNA^{Leu}$(GAG) in filter binding reaction at 4°C[a]

LeuRS	k_d (μM)
*Nm*LeuRS1	6.36 ± 1.17
*Nm*LeuRS2	3.36 ± 0.89

[a]The results are the average of three independent repeats with standard deviations indicated.

by *Nm*LeuRS1 was similar to that of *Ph*LeuRS, both depending on the conserved Ile residue (Ile902 and Ile966 for *Nm*LeuRS1 and *Ph*LeuRS, respectively) (Figure 4A) (26). Moreover, complete deletion of the CTD (*Nm*LeuRS1-ΔCTD) led to the total loss of aminoacylation activity (Figure 4B), indicating the importance of the archaeal CTD in the *Nm*LeuRS1 aminoacylation reaction.

We then explored the recognition mode based on analysis of $tRNA^{Leu}$. Sequence alignment of $tRNA^{Leu}$s showed that A47c and G47d at the tip of the long variable loop were absolutely conserved in archaea (Supplementary Figure S2). These residues have been identified as the sequence-specific determinants in archaeal *H. volcanii* $tRNA^{Leu}$ (*Hv*$tRNA^{Leu}$) and *Ph* $tRNA^{Leu}$ (25,26). Mutations of A47c and G47d to the other three nucleotides in *Nm*$tRNA^{Leu}$(GAG) were performed to obtain *Nm*$tRNA^{Leu}$(GAG)-A47cC, -A47cG, -A47cU, -G47dA, -G47dC and -G47dU, respectively. None of the mutants were efficiently aminoacylated by *Nm*LeuRS1 except *Nm*$tRNA^{Leu}$(GAG)-A47cC, which retained 7% of the catalytic activity of the wild-type $tRNA^{Leu}$ (Figure 4C, Supplementary Table S1). Therefore, like archaeal *Ph*$tRNA^{Leu}$ and *Hv*$tRNA^{Leu}$, the A47c and G47d bases located in the tip of the long variable loop were of great importance in the recognition process.

These results showed that *Nm*LeuRS1 distinguished *Nm*$tRNA^{Leu}$ via a similar mechanism to that used by archaeal *Ph*LeuRS with the last few residues of enzyme (especially conserved Ile902) and the conserved A47c and G47d residues of $tRNA^{Leu}$ being crucial elements for recognition. As *Nm*LeuRS1 also possesses bacterial aminoacylation and editing domains, the question of whether these two domains conferred the ability to recognize bacterial $tRNA^{Leu}$s on *Nm*LeuRS1 remained unresolved. To address this issue, the aminoacylation activity of *Nm*LeuRS1 for bacterial *Ec*$tRNA^{Leu}$ (the Leu accepting activity was 1600 pmol/A_{260}) and archaeal *Ph*$tRNA^{Leu}$ was determined. *Nm*LeuRS1 was able to charge archaeal *Ph*$tRNA^{Leu}$ but not bacterial *Ec*$tRNA^{Leu}$ (Table 2, Figure 4D), implying that the bacterial aminoacylation and editing domains contributed little to tRNA species specificity. On the other hand, *Ec*LeuRS was only able to charge its cognate *Ec*$tRNA^{Leu}$ but not *Nm*$tRNA^{Leu}$ and *Ph*$tRNA^{Leu}$ (Figure 4E). Cross-activation of these $tRNA^{Leu}$s by *Nm*LeuRS2 was also evaluated, and similar results were obtained (Figure 4F), suggesting that both *Nm*LeuRSs distinguished $tRNA^{Leu}$s in the archaeal mode. In addition, we replaced the CTD (Thr759-Asp904) of *Nm*LeuRS1 with its *Ec*LeuRS counterpart (Asp791-Gly860) to generate *Nm*LeuRS1-*Ec*CTD to mimic a complete bacterial LeuRS. However, *Nm*LeuRS1-*Ec*CTD failed to aminoacylate *Ec*$tRNA^{Leu}$, *Ph*$tRNA^{Leu}$ and *Nm*$tRNA^{Leu}$ (Supplementary Figure S5), indicating that the archaeal CTD plays a key role in archaeal $tRNA^{Leu}$ recognition and that fusion of a bacterial CTD with the basis of bacterial region of *Nm*LeuRS1 failed to reinstate bacterial $tRNA^{Leu}$ aminoacylation capacity.

Taken together, these lines of evidence suggested that *Nm*LeuRS1 distinguished *Nm*$tRNA^{Leu}$ in the archaeal mode and indicated that the archaeal CTD, but not the bacterial aminoacylation and editing domains of *Nm*LeuRS1, contributed its archaeal tRNA recognition capacity.

The N-terminal region of *Nm*LeuRS1 is of bacterial type

To explore whether the N-terminal region of *Nm*LeuRSs was of bacterial type, we constructed several mutations in amino acid residues of *Nm*LeuRS1, only conserved in bacterial but not archaeal/eukaryotic LeuRSs. Asp95 and Gln207 of *Nm*LeuRS1 were equivalent to Asp80 and Gln190 in *Ec*LeuRS, which, respectively, interacted with A76 and C74 of *Ec*$tRNA^{Leu}$ during aminoacylation reaction, as showed in its 3D structure (PDB: 4AQ7) (Figure 5A) (21), and conserved in only bacterial but not archaeal/eukaryotic LeuRSs (Figure 5B), suggesting they might play a key role in the aminoacylation activity of bacterial LeuRS. We obtained *Nm*LeuRS1-D95A and -Q207E mutants, which would disturb the interaction of LeuRS and $tRNA^{Leu}$.

The results showed that the mutant *Nm*LeuRS1-D95A abolished all the aminoacylation activity and *Nm*LeuRS1-Q207E only retained half of the

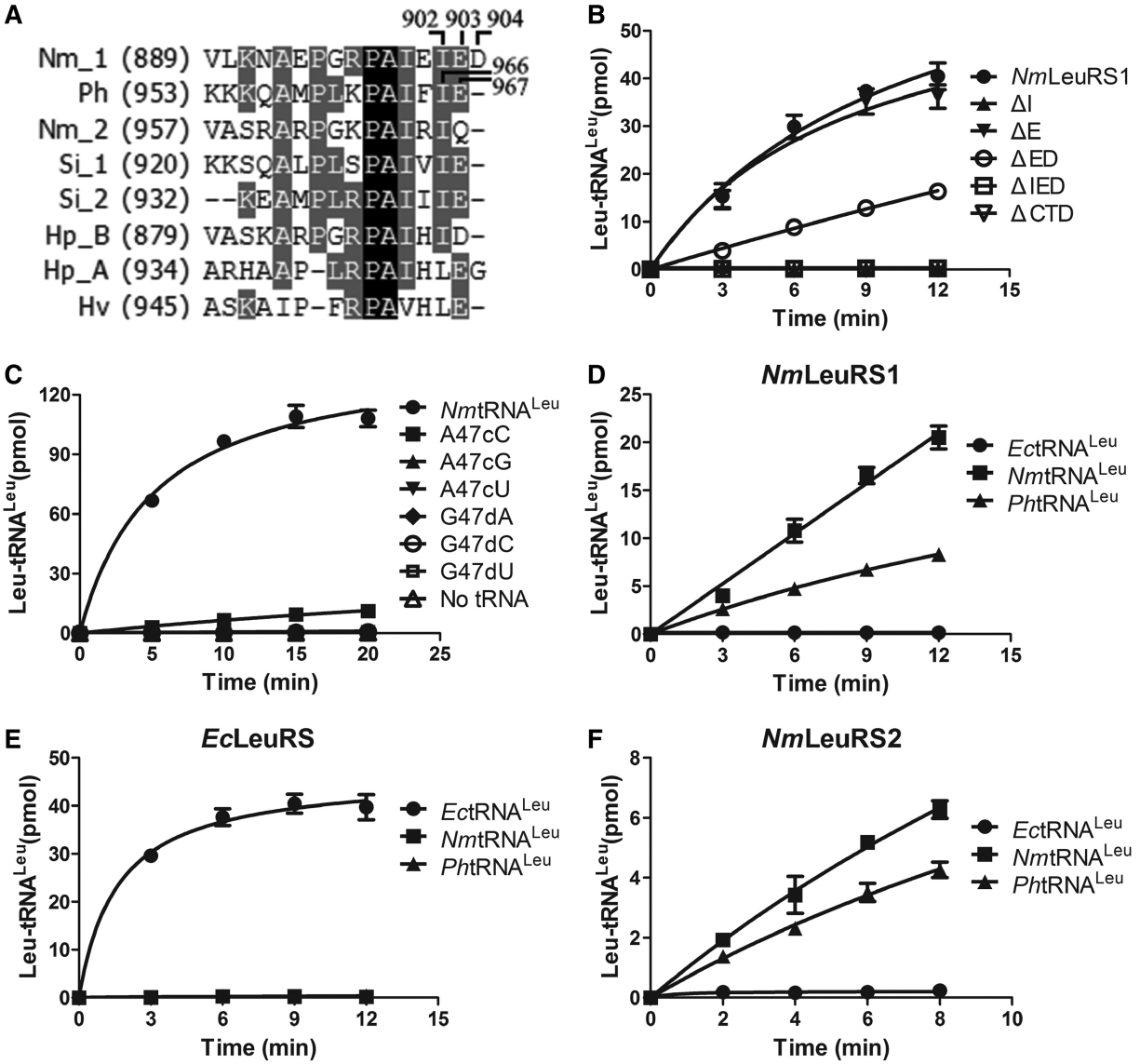

Figure 4. *Nm*LeuRSs discriminate *Nm*tRNA^{Leu} in archaeal mode. (**A**) Sequence alignment of the C-terminus of different LeuRSs. Nm_1 and Nm_2, *N. magadii* LeuRS1 and LeuRS2; Ph, *P. horikoshii*; Si_1 and Si_2, *S. islandicus* LeuRS [LeuRS1 (accession No. YP_002829648.1) and LeuRS2 (accession No. YP_002829589.1)]; Hp_B and Hp_A, *H. paucihalophilus* LeuRS [bacterial type (accession No. WP_007982262.1) and archaeal type (accession No. WP_007982263.1)]; Hv, *H. volcanii*. (**B**) The aminoacylation activities of 500 nM *Nm*LeuRS1 (black circle), 500 nM *Nm*LeuRS1-ΔI (black up-pointing triangle), 500 nM *Nm*LeuRS1-ΔE (black down-pointing triangle), 500 nM *Nm*LeuRS1-ΔED (white circle), 500 nM *Nm*LeuRS1-ΔIED (white square) and 500 nM *Nm*LeuRS1-ΔCTD (white down-pointing triangle) for 5.6 μM *Nm*tRNA^{Leu}(GAG). (**C**) The aminoacylation activities of 500 nM *Nm*LeuRS1 for 12 μM (0.3 μg/μl) *Nm*tRNA^{Leu}(GAG) (black circle), 0.3 μg/μl *Nm*tRNA^{Leu}-A47cC (black square), 0.3 μg/μl *Nm*tRNA^{Leu}-A47cG (black up-pointing triangle), 0.3 μg/μl *Nm*tRNA^{Leu}-A47cU (black down-pointing triangle), 0.3 μg/μl *Nm*tRNA^{Leu}-G47dA (black diamond), 0.3 μg/μl *Nm*tRNA^{Leu}-G47dC (white circle) and 0.3 μg/μl *Nm*tRNA^{Leu}-G47dU (white square); the cross-species aminoacylation activities of 200 nM *Nm*LeuRS1 (**D**), 10 nM *Ec*LeuRS (**E**) and 3 μM *Nm*LeuRS2 (**F**) for 4 μM *Ec*tRNA^{Leu} (black circle), 4 μM *Nm*tRNA^{Leu} (black square) and 4 μM *Ph*tRNA^{Leu} (black up-pointing triangle), respectively.

aminoacylation activity compared with *Nm*LeuRS1 (Figure 5C), suggesting the bacterial type of the N-terminal region of *Nm*LeuRS1.

In addition, zinc binding domains (ZN domain) were conserved in many class I tRNA synthetase. However, besides the universal ZN-1 domain, only bacterial/mitochondrial but not archaeal/eukaryotic LeuRSs contained the ZN-2 domain (48). It has shown that mutations of conserved Cys residues in ZN domain obviously reduced the aaRS activities and the growth of cells (49,50). Sequence analysis showed the ZN-2 domain existed in both *Nm*LeuRSs as most bacterial LeuRSs (Figure 5B). Therefore, we performed the mutations of Cys to Ala at ZN-2 domain of *Nm*LeuRS1 to produce double mutants *Nm*LeuRS1-C448A/C452A and -C488A/C491A. The results showed both mutants totally lost their aminoacylation activities (Figure 5C), indicating the crucial role of bacterial LeuRS-specific ZN-2 domain and further supporting our suggestion that the N-terminal region of *Nm*LeuRS1 was of bacterial type.

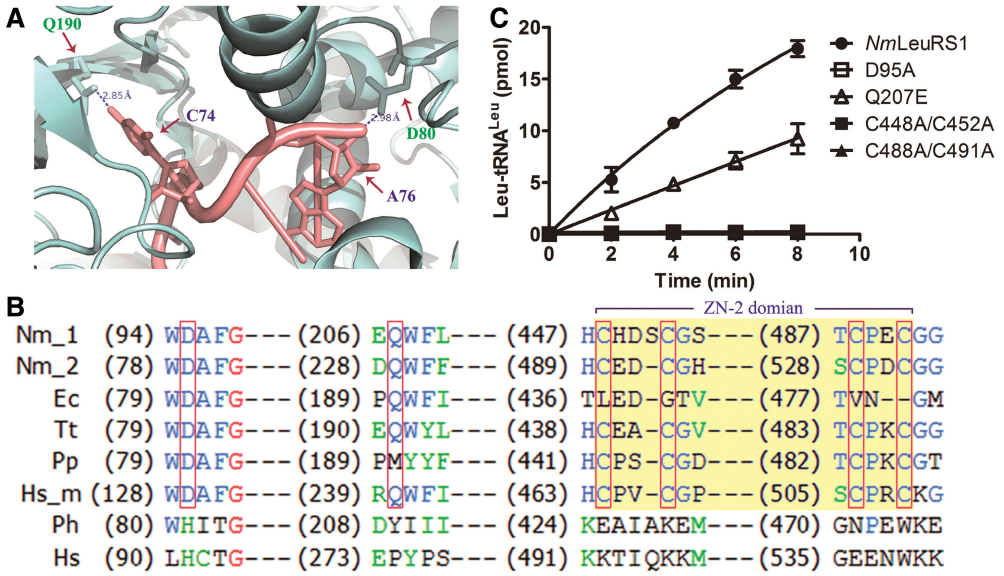

Figure 5. The N-terminal region of *Nm*LeuRS1 is of bacterial type. (**A**) The structure of *Ec*LeuRS complex with $tRNA^{Leu}$ in aminoacylation conformation [PDB code 4AQ7, (21)]. *Ec*LeuRS is gray colored and the tRNA molecule is in salmon. The residues D80, Q190 in *Ec*LeuRS (equivalent to D95, Q207 in *Nm*LeuRS1) and the respectively interacted nucleotides A76, C74 are indicated. (**B**) Sequence alignment of the N-terminal region of different LeuRSs. The red boxes and the yellow block indicate the specific residues and the ZN-2 domain investigated in this study. Nm_1 and Nm_2, *N. magadii* LeuRS1 and LeuRS2; Ec, *E. coli*; Tt, *Thermus thermophilus*; Pp, *Pseudomonas putida*; Hs_m, *H. sapiens* mitochondrial LeuRS; Ph, *P. horikoshii*; Hs, *H. sapiens*. (**C**) The aminoacylation activities of 200 nM *Nm*LeuRS1 (black circle), 200 nM *Nm*LeuRS1-D95A (white square), 200 nM *Nm*LeuRS1-Q207E (white up-pointing triangle), 200 nM *Nm*LeuRS1-C448A/C452A (black square) and 200 nM *Nm*LeuRS1-C488A/C491A (black up-pointing triangle) for 4 μM *Nm*$tRNA^{Leu}$ (GAG).

*Nm*LeuRS1 misactivates several non-cognate amino acids

LeuRSs are characterized by the capacity to activate a wide range of amino acids that are structurally similar to cognate Leu (30,35). We determined the amino acid activation activity of *Nm*LeuRS1 toward non-cognate Ile and Met as well as the non-proteinogenic amino acids Nva and ABA. Nva and ABA were misactivated by *Nm*LeuRS1, whereas the kinetic constants of Ile and Met could not be determined because kinetic analysis at high concentrations of Ile and Met was not realized. The k_{cat} of *Nm*LeuRS1 for Nva ($0.364 \pm 0.008\ s^{-1}$) and ABA ($0.518 \pm 0.028\ s^{-1}$) activation were ~60 and 90% of that for cognate Leu ($0.563 \pm 0.012\ s^{-1}$), although the K_m values for Nva (955 ± 22 μM) and ABA ($37\,820 \pm 1630$ μM) were much higher compared with that of cognate Leu (8.43 ± 1.3 μM) (Table 4). For ABA, the discrimination factor (DF) was 1/4912, which was lower than the mistranslation frequency (1/3000) of protein biosynthesis (6). In contrast, *Nm*LeuRS1 has to clear the misactivated Nva (DF: 1/175) by its editing activity. Because of the extremely low amino acid activation activity of *Nm*LeuRS2 even toward cognate Leu, accurate evaluation of the kinetics of misactivation for non-cognate amino acids was not achieved.

*Nm*LeuRS1 exhibits obvious post-transfer editing activity to prevent generation of mischarged $tRNA^{Leu}$

*Nm*LeuRS1 has the bacterial Rossmann fold aminoacylation and editing domains, which means that the orientation and the insertion point of the CP1 editing domain into the Rossmann fold is totally different from its archaeal counterparts, such as the CP1 domain of *Ph*LeuRS (14). However, it has the normal archaeal CTD for $tRNA^{Leu}$ binding. Therefore, whether the editing activity of the bacterial CP1 domain and the $tRNA^{Leu}$ binding capacity of the archaeal CTD coordinate to mediate post-transfer editing is an interesting question. To confirm the editing activity of *Nm*LeuRS1, the post-transfer editing essential Asp residue (Asp354 of *Nm*LeuRS1), as revealed in various LeuRS systems (14,30, 35,51,52), was mutated to Ala residue to generate *Nm*LeuRS1-D354A. To monitor the post-transfer editing directly, misacylated Nva-[^{32}P]*Nm*$tRNA^{Leu}$ was produced by *Ph*LeuRS1-D332A (14). The hydrolysis of Nva-*Nm* $tRNA^{Leu}$ showed that only *Nm*LeuRS1 was able to deacylate the misacylated product (Figure 6). In contrast, *Nm*LeuRS1-D354A lost its editing ability (Figure 6A and B). We also analyzed the editing activity of *Nm*LeuRS2 in a similar manner; however, both wild-type *Nm*LeuRS2 and the mutant of the conserved Asp390 (*Nm*LeuRS2-D390A)

Table 4. Amino acid activation kinetics of *Nm*LeuRS1 for Leu, Nva and ABA[a]

Amino acids	K_m (μM)	k_{cat} (s^{-1})	k_{cat}/K_m ($mM^{-1}\,s^{-1}$)	Discriminate factor (DF)[b]
Leu	8.43 ± 1.3	0.563 ± 0.012	66.8	1
Nva	955 ± 22	0.364 ± 0.008	0.381	1/175
ABA	37 820 ± 1630	0.518 ± 0.028	0.0136	1/4912

[a]The results are the average of three independent repeats with standard deviations indicated.
[b]DF is defined as the relative ratio of k_{cat}/K_m for non-cognate amino acids compared with that for Leu.

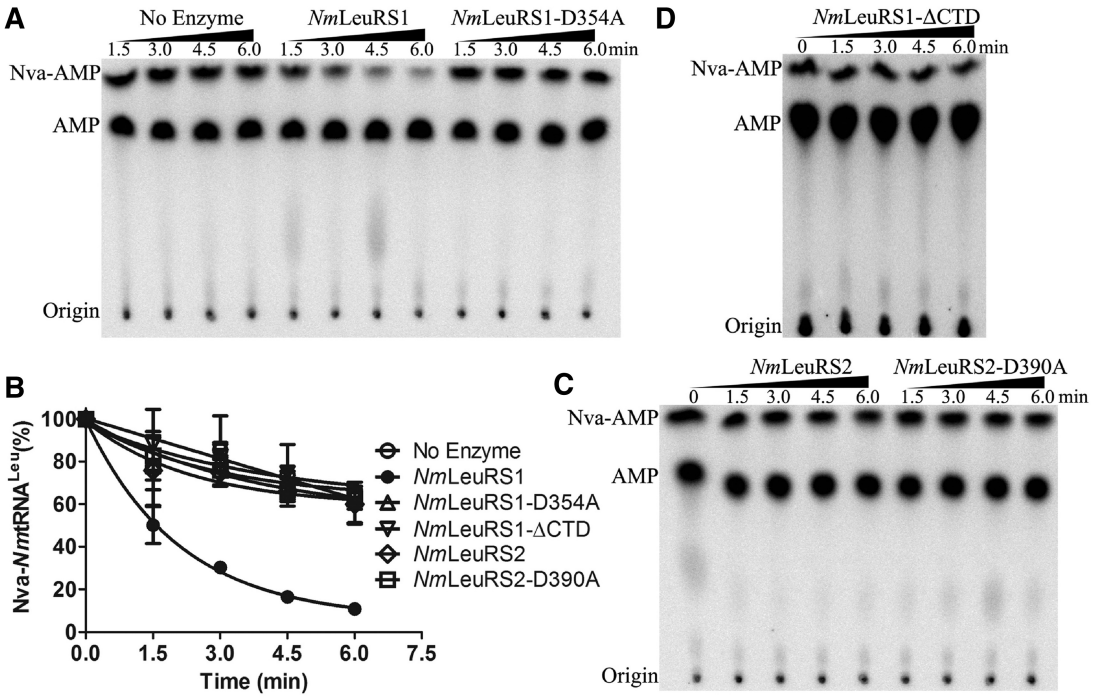

Figure 6. *Nm*LeuRS1 but not *Nm*LeuRS2 deacylates Nva-*Nm*tRNA^{Leu}. (**A**) Representative graph showing the post-transfer editing activity of 500 nM *Nm*LeuRS1 and 500 nM *Nm*LeuRS1-D354A based on TLC assay. (**B**) Quantification of the deacylation activities of *Nm*LeuRS (black circle), *Nm*LeuRS1-D354A (white up-pointing triangle), *Nm*LeuRS1-ΔCTD (white down-pointing triangle), *Nm*LeuRS2 (white diamond) and *Nm*LeuRS2-D390A (white square) in A, C and D. Representative graphs showing the post-transfer editing activity of 500 nM *Nm*LeuRS2 and 500 nM *Nm*LeuRS2-D390A (**C**), 500 nM *Nm*LeuRS1-ΔCTD (**D**) based on TLC assay.

exhibited no editing capacity (Figure 6B and C), suggesting the post-transfer editing of *Nm*LeuRS2 was lost or too weak to be detected in deacylation assays.

Whether *Hh*LeuRSs exhibited similar results with *Nm*LeuRSs in deacylation activities was then explored. Our data revealed that although both *Hh*LeuRSs could deacylate mischarged Nva-*Hh*tRNA^{Leu}, but *Hh*LeuRS2 showed weaker activity than *Hh*LeuRS1. These further confirmed the phenomena that an active LeuRS and an inactive (or slightly active) one coexisted in halobacteria (Supplementary Figure S4D and E).

Previous work also showed that the editing activity of *Ph*LeuRS was not altered by deletion of the CTD (14). Therefore, to investigate the editing function of the archaeal CTD of *Nm*LeuRS1, the *Nm*LeuRS1-ΔCTD mutant was generated and shown to exhibit a complete loss of deacylation activity (Figure 6B and D). This suggested that the archaeal CTD of *Nm*LeuRS1, unlike that of *Ph*LeuRS, coordinated with its CP1 domain to play a key role in post-transfer editing.

We then determined the misacylation activity of *Nm*LeuRSs. The result showed no Ile and little Met could be misloaded to *Nm*tRNA^{Leu} by *Nm*LeuRSs (Supplementary Figure S6). In addition, *Nm*LeuRS1-D354A produced significantly more (~3-fold) Nva-*Nm*tRNA^{Leu} and 30% more ABA-*Nm*tRNA^{Leu} compared with wild-type *Nm*LeuRS1 (Figure 7A and B), suggesting the essential editing role of *Nm*LeuRS1 in preventing the synthesis of mischarged tRNA^{Leu}. However, the amount of generated Nva-*Nm*tRNA^{Leu} and ABA-*Nm*tRNA^{Leu} was comparable with wild-type *Nm*LeuRS2 and mutant *Nm*LeuRS2-D390A (Figure 7C and D), which is consistent with the observation that post-transfer editing was lost or significantly impaired in both enzymes (Figure 6B and C). In addition, it is notable that wild-type *Nm*LeuRSs were able to synthesize trace amount of Nva-tRNA^{Leu} and an obvious amount of ABA-tRNA^{Leu}. This is also the case for *Candida albicans* LeuRS (*Ca*LeuRS) (30), suggesting that editing capacity is insufficient for proofreading non-cognate amino acids at saturated concentrations. It can be speculated that the paradox between ABA misaminoacylation and charging accuracy can be accounted for by fine discrimination against ABA at the aminoacylation active site (1/4912) as proposed for *Ca*LeuRS (30).

Editing characteristics of *Nm*LeuRS1

On the basis of the efficient editing activity of *Nm*LeuRS1, we further investigated the editing characteristics of *Nm*LeuRS1 in TLC-based AMP formation assays on the basis that a single AMP molecule is released by either the hydrolysis of misactivated aa-AMP by pre-transfer editing or in the cycle of misacylation and post-transfer editing; therefore, measurement of the released AMP in the TLC assay can be used to quantify the editing capacity (53).

In the presence of *Nm*tRNA^{Leu}, the observed rate constant (k_{obs}) of AMP formation by *Nm*LeuRS1 was $(8.74 \pm 0.36) \times 10^{-2}\,s^{-1}$ (Figure 8A, Table 5), which represented the global editing activity. In the absence of *Nm*tRNA^{Leu}, the AMP formation rate was $(1.00 \pm 0.13) \times 10^{-2}\,s^{-1}$, ~11.4% of that in the presence of

*Nm*tRNA^{Leu} (1.00/8.74). This result suggested that tRNA-independent pre-transfer editing contributed little to the total editing activity. Theoretically, the enhanced AMP formation activity, as a result of tRNA addition, may be derived from tRNA-dependent pre-transfer editing and/or post-transfer editing. To distinguish these two pathways, we analyzed AMP formation using *Nm*LeuRS1-D354A. The k_{obs} of *Nm*LeuRS1-D354A in the presence of tRNA was $(3.40 \pm 0.19) \times 10^{-2}\,s^{-1}$ (Figure 8B, Table 5), indicating that tRNA-dependent pre-transfer editing contributed ~27.5% to the total editing activity [(3.40 – 1.00)/8.74]. Taken together, these results demonstrate that post-transfer editing contributed more than half (61.1%) of the Nva editing activity [(8.74 – 3.40)/8.74].

In addition, if the editing activities failed to clear all the misproducts, Nva-AMP should be detected in the TLC assays. In the presence of *Nm*tRNA^{Leu}, the *Nm*LeuRS1-D354A mutant still failed to clear all the misproducts (with obvious accumulation of Nva-AMP) (Figure 8B) in contrast to *Nm*LeuRS1 with tRNA^{Leu} (without obvious accumulation of Nva-AMP), suggesting that pre-transfer editing is not sufficient for maintaining the catalytic fidelity. Only the wild-type *Nm*LeuRS1, which has post-transfer editing in the presence of *Nm*tRNA^{Leu}, efficiently prevented the accumulation of Nva-AMP (Figure 8A).

DISCUSSION

Unique LeuRS models identified to date

There are several interesting examples of LeuRSs with unique features with regard to primary or tertiary structure. For example, in *A. aeolicus*, LeuRS is no longer a single polypeptide but rather a heterodimeric enzyme (αβ-LeuRS), although no advantage associated with this structure has been identified (34). However, both α and β subunits are of bacterial origin. In *Mycoplasma mobile*, LeuRS is naturally devoid of the CP1 editing domain (54). This is the first example of a truncated LeuRS, leading to an error-prone synthetase. Consequently, *M. mobile* exhibits genetic code ambiguity in its proteome, which might be advantageous for avoiding host immune defense (55). In addition, human mitochondrial LeuRS contains a naturally degenerated CP1 domain (56), which suggests a degenerate editing activity. However, mitochondrial LeuRS exhibited a fine discrimination capacity toward cognate Leu and non-cognate amino acids in the amino activation step. The reason for this degeneration has not been definitely identified. This work describes a unique example of a LeuRS/tRNA^{Leu} system, in which two chimeric LeuRSs coexist in a single cell compartment. Furthermore, we show that *Nm*LeuRSs distinguish *Nm*tRNA^{Leu} in the archaeal mode.

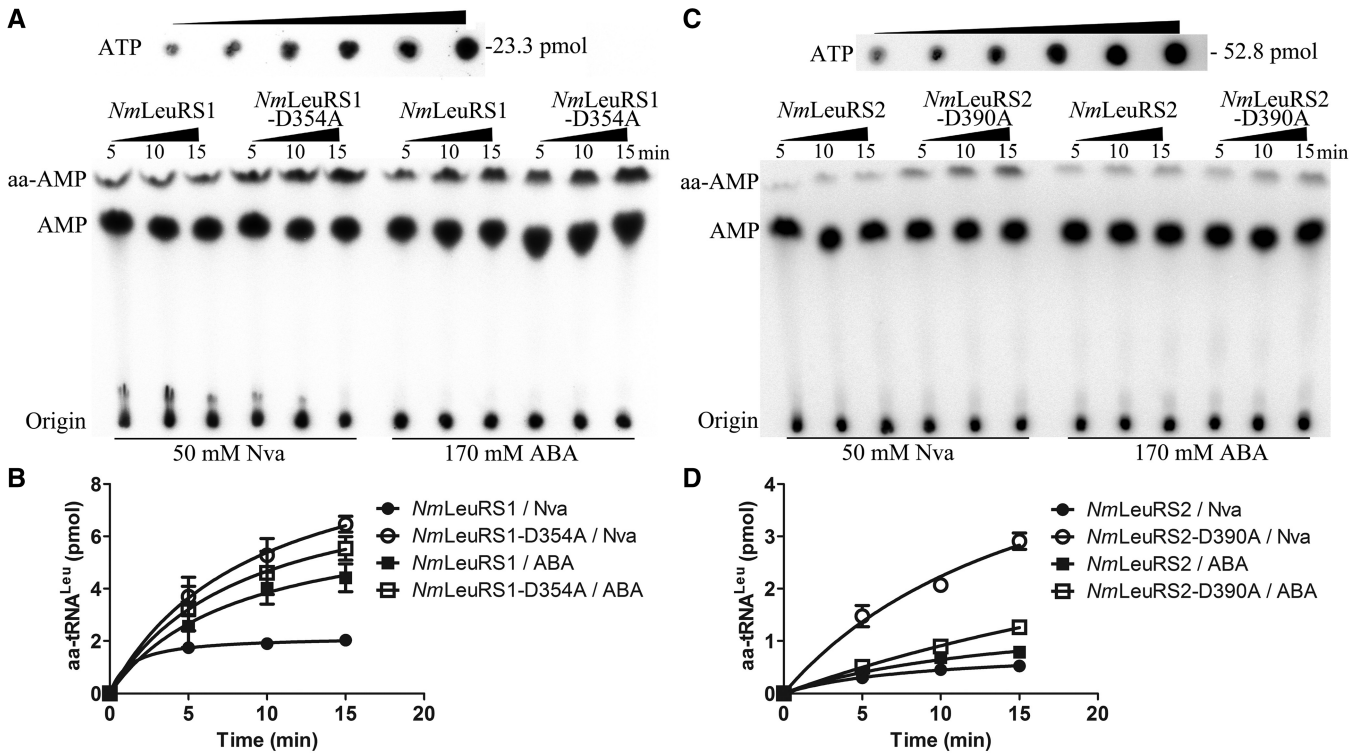

Figure 7. *Nm*LeuRSs misacylate *Nm*tRNA^{Leu} with Nva and ABA. (**A**) Representative image showing the misacylation activities of 500 nM *Nm*LeuRS1 and 500 nM *Nm*LeuRS1-D354A for Nva and ABA based on TLC assay. A 2-fold diluted [α-^{32}P]ATP for quantification (initial, 52.8 pmol) is also shown. (**B**) Quantification of the misacylation activities of *Nm*LeuRS1 [for Nva (black circle), for ABA (black square)] and *Nm*LeuRS1-D354A [for Nva (white circle), for ABA (white square)] in A. (**C**) Representative image showing the misacylation activities of 2 μM *Nm*LeuRS2 and 2 μM *Nm*LeuRS2-D390A for Nva and ABA based on TLC assay. (**D**) Quantification of the misacylation activities of *Nm*LeuRS2 [for Nva (black circle), for ABA (black square)] and *Nm*LeuRS2-D390A [for Nva (black square), for ABA (white square)] in C.

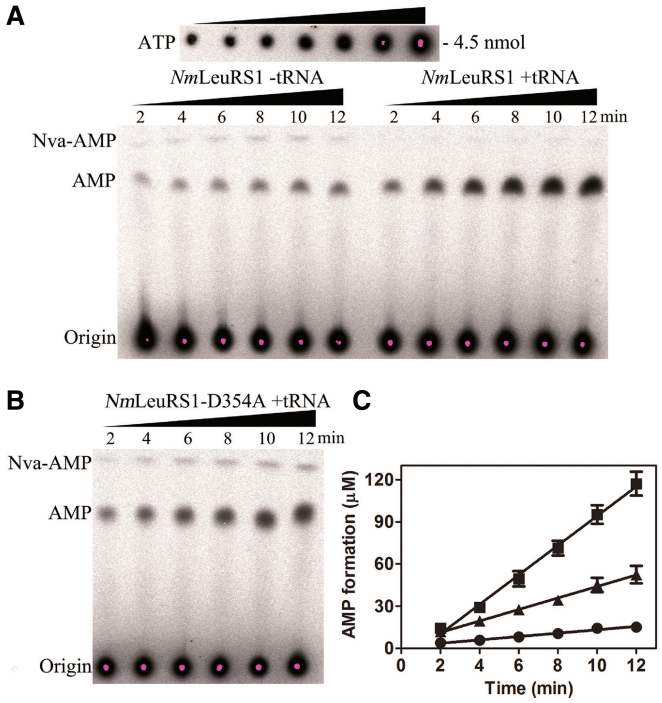

Figure 8. The editing properties for Nva by *Nm*LeuRS1. (**A**) A representative image showing the formation of [^{32}P]AMP by 2 μM *Nm*LeuRS1 in the absence (− tRNA) or presence (+ tRNA) of 25 μM *Nm*tRNA^{Leu}. A 2-fold diluted [α-^{32}P]ATP for quantification (initial concentration, 4.5 nmol) is also shown. (**B**) A representative image showing the formation of [^{32}P]AMP by *Nm*LeuRS1-D354A in the presence of *Nm*tRNA^{Leu}. (**C**) Quantification of the formation of [^{32}P]AMP by *Nm*LeuRS1without tRNA (black circle) and with tRNA (black square) and by *Nm*LeuRS1-D354A with tRNA (black up-pointing triangle).

Table 5. The k_{obs} of *Nm*LeuRS1 and *Nm*LeuRS1-D354A in AMP formation with Nva[a]

	*Nm*tRNA^{Leu}(GAG)	k_{obs} (s^{-1})
*Nm*LeuRS1	−	$(1.00 \pm 0.13) \times 10^{-2}$
	+	$(8.74 \pm 0.36) \times 10^{-2}$
*Nm*LeuRS1-D354A	+	$(3.40 \pm 0.19) \times 10^{-2}$

[a]The results are the average of three independent repeats with standard deviations indicated.

Coexistence of two aaRSs in a single compartment

There are sporadic examples of the existence of dual aaRS activities in a single cell compartment. In human cytoplasm, two arginyl-tRNA synthetases (ArgRSs) are derived from two translational initiation sites by a single messenger RNA (57). The short ArgRS is proposed to participate in modification at the N-terminus of proteins targeted for degradation by providing the substrate for argninyl-tRNA transferase (58). Moreover, higher eukaryotes encode two threonyl-tRNA synthetases. Sequence analysis and genetic studies have shown that the short form generates Thr-tRNA^{Thr} for human cytoplasmic protein biosynthesis, whereas the significance of the longer isoform remains to be clarified (53). The coexistence of two types of glycyl-tRNA synthetase (GlyRS, *Sc*GlyRS1 and *Sc*GlyRS2) has been reported in *S. cerevisiae*. *Sc*GlyRS1 is responsible for both cytoplasmic and mitochondrial activities, whereas GlyRS2 is dysfunctional and not essential for growth (59). Many bacterial species, such as *Helicobacter pylori*, also contain two duplicated glutamyl-tRNA synthetase (GluRS, *Hp*GluRS1 and *Hp*GluRS2). It has been revealed that *Hp*GluRS1 acylated only tRNA^{Glu}; whereas *Hp*GluRS2 was specific solely for tRNA^{Gln} (60). In addition, two types of cytoplasmic LeuRSs have been reported in *Agrobacterium radiobacter* K84 (61), in which a second non-essential LeuRS (AgnB2) is encoded by the pAgK84 plasmid, in addition to the essential genomic form. The activity of the genomic form can be inhibited by TM 84, which is synthetized to kill *Agrobacterium tumefaciens*, which causes crown gall tumors in plants by specific inhibition of LeuRS activity. AgnB2 LeuRS, which is non-sensitive to TM 84, works as a self-protective copy.

Considering the obviously high aminoacylation and editing activity of *Nm*LeuRS1, we propose that *Nm*LeuRS1 is responsible for Leu-tRNA^{Leu} generation. However, both the aminoacylation and editing activities of *Nm*LeuRS2 were significantly lower than those of *Nm*LeuRS1; therefore, *Nm*LeuRS2 may be not essential for protein biosynthesis. Compared with *Nm*LeuRS1 and other bacterial LeuRSs, there are several substitutions at key amino acids (such as Ser631 instead of Lys in the catalysis-essential KMSKS motif) or insertion in the Rossmann-fold amino acid activation domain in *Nm*LeuRS2 [such as a 38-aa insertion (Glu174-Thr211), Supplementary Figure S1A]. These changes may, individually or collectively, have some direct or indirect influence on the activity of *Nm*LeuRS2. Unfortunately, substitutions of these conserved residues with the corresponding sites in *Ec*LeuRS (such as Ser631 to Lys631 to regenerate the KMSKS motif) or deletion of the 38-aa insertion in *Nm*LeuRS2 failed to restore its amino acid activation and aminoacylation activities (data not shown).Therefore, the detailed mechanism underlying the loss of *Nm*LeuRS2 activity requires further investigation.

In contrast, *Nm*LeuRS2 retained the affinity for *Nm*tRNA^{Leu}, indicating *Nm*LeuRS2 mediates other functions in a tRNA-dependent manner. Many aaRS-like proteins are responsible for tRNA-dependent *trans*-editing activities rather than the *cis*-editing domains, such as human ProX for Ala-tRNA^{Pro}, AlaXp for Ser-tRNA^{Ala} and Gly-tRNA^{Ala}, ThrXp for Ser-tRNA^{Thr} and Ybak for Cys-tRNA^{Pro} (9). However, the undetectable editing activity of *Nm*LeuRS2 may exclude such a possibility. It is also possible that the editing function of *Nm*LeuRS2 relies on other cofactors. Other studies revealed that a lysyl-tRNA synthetase-like protein PoxA modifies elongation factor-P with (R)-β-lysine and that a SerRS-like insect mitochondrial protein is also a tRNA-binding protein without aminoacylation activity but with an essential mitochondrial function (62,63). Therefore, it can be speculated that *Nm*LeuRS2 functions in other pathways besides tRNA aminoacylation.

Chimeric characteristics of *Nm*LeuRSs

Most archaea, such as *P. horikoshii*, harbor only one archaeal LeuRS gene. However, *N. magadii*, *H. paucihalophilus* and *S. islandicus* are extremophilic archaea, all of which contain two *leuS* genes. Sequence alignment revealed that the CTD in these LeuRSs are all of the archaeal type (Supplemental Figure S1B), suggesting the same archaeal recognition mode. However, the N-terminal region (including the Rossmann-fold, the CP1 domain and the α-helix bundle domain) is different. Specifically, the N-terminal regions of both *Nm*LeuRSs are bacterial type (Supplemental Figure S1A), but the counterparts [Met1-Pro781 in the LeuRS (accession No. YP_002829648.1), Met1-Pro792 in another LeuRS (accession No. YP_002829589.1)] of both *S. islandicus* LeuRSs are archaeal type. In contrast, the N-terminal region [Met1-Pro746 in the LeuRS (accession No. WP_007982262.1)] of one *H. paucihalophilus* LeuRS (*Hp*LeuRS) is bacterial type, whereas the other [Met1-Pro790 in another *Hp*LeuRS (accession No. WP_007982263.1)] is archaeal type. This phenomenon indicates the complex distribution pattern of LeuRSs in the archaeal world. The functional detail of both *S. islandicus* LeuRSs and *Hp*LeuRSs requires investigation.

Based on the complicated distribution of LeuRS in these species, we propose that the ancestor of most archaeal species encoded only one archaeal LeuRS. However, an ancient horizontal gene transfer of bacterial LeuRS occurred from an organism related to the bacterial ancestor to the haloarchaea. In some cases, such as in *N. magadii*, gene fusion may have occurred between the original archaeal LeuRS and the transferred bacterial LeuRS, leading to the presence of a chimeric LeuRS with the N-terminal region replaced by the bacterial counterpart. This new isoform coexists with the original archaeal copy. The bacterial form of LeuRS (or the newly generated chimeric LeuRS) further underwent gene duplications (64) and/or horizontal gene transfers (65) within the haloarchaea. It is possible that this new bacterial or chimeric LeuRS provided advantages in participating in the translational machinery in those species and thus, the original archaeal LeuRS copy was lost subsequently.

Despite the divergence of the N-terminal region of archaeal LeuRSs, all archaeal LeuRSs contain a similar archaeal CTD, suggesting the essential role of this domain in recognizing archaeal $tRNA^{Leu}$s. The specific *Nm*LeuRS/$tRNA^{Leu}$ interaction mode strongly suggests that tRNA synthetases are able to evolve to adapt to the tRNAs and thus provides a striking example of coevolution between tRNA synthetase/tRNA. We showed that the CTD of *Nm*LeuRS1 was essential for both aminoacylation and editing reactions, confirming its crucial role in Leu-$tRNA^{Leu}$ synthesis and translational quality control. Furthermore, substitution of archaeal CTD with bacterial CTD totally abolished aminoacylation (Supplementary Figure S5) and editing activities (data not shown), which is consistent with its maintenance of the archaeal CTD. Considering that *Ec*LeuRS lost its aminoacylation activity in high KCl solution (Figure 3B), we cannot rule out the potential possibility that the bacterial CTD in swapping mutant could not fold correctly in reaction buffer. For *Nm*LeuRS1, it is also possible that the archaeal CTD prevents misacylation of $tRNA^{Ile}$ as revealed in the *Ph*LeuRS system (66).

In summary, our data reveal the haloalkaliphilic nature of *Nm*LeuRSs and further elucidate the aminoacylation and editing activities of *Nm*LeuRSs as well as the function of CTD in both the recognition and editing of *Nm*$tRNA^{Leu}$. Thus, this study provides a comprehensive characterization of the aaRS/tRNA system in halobacteria.

SUPPLEMENTARY DATA

Supplementary Data are available at NAR Online.

ACKNOWLEDGEMENTS

The authors thank Profs. Li Huang and Hua Xiang and Drs Li Guo and Da-He Zhao (Institute of Microbiology, Beijing, China) for providing us *N. magadii* ATCC 43099 and *H. hispanica* ATCC 33960 genomic DNA. They are also grateful to Dr Yuchen Liu (Department of Molecular Biophysics and Biochemistry, Yale University) for valuable suggestions. The authors gratefully acknowledge the support of SA-SIBS scholarship program.

FUNDING

National Key Basic Research Foundation of China [2012CB911000]; Natural Science Foundation of China [31130064, 31270852]. Funding for open access charge: [2012CB911000].

Conflict of interest statement. None declared.

REFERENCES

1. Lucas-Lenard,J. and Lipmann,F. (1971) Protein biosynthesis. *Annu. Rev. Biochem.*, **40**, 409–448.
2. Ibba,M. and Söll,D. (2000) Aminoacyl-tRNA synthesis. *Annu. Rev. Biochem.*, **69**, 617–650.
3. Cusack,S., Berthet-Colominas,C., Hartlein,M., Nassar,N. and Leberman,R. (1990) A second class of synthetase structure revealed by X-ray analysis of *Escherichia coli* seryl-tRNA synthetase at 2.5 Å. *Nature*, **347**, 249–255.
4. Eriani,G., Delarue,M., Poch,O., Gangloff,J. and Moras,D. (1990) Partition of tRNA synthetases into two classes based on mutually exclusive sets of sequence motifs. *Nature*, **347**, 203–206.
5. Zhou,X. and Wang,E. (2013) Transfer RNA: a dancer between charging and mis-charging for protein biosynthesis. *Sci. China Life Sci.*, **56**, 921–932.
6. Loftfield,R.B. and Vanderjagt,D. (1972) The frequency of errors in protein biosynthesis. *Biochem. J.*, **128**, 1353–1356.
7. Chen,J.F., Guo,N.N., Li,T., Wang,E.D. and Wang,Y.L. (2000) CP1 domain in *Escherichia coli* leucyl-tRNA synthetase is crucial for its editing function. *Biochemistry*, **39**, 6726–6731.
8. Dock-Bregeon,A., Sankaranarayanan,R., Romby,P., Caillet,J., Springer,M., Rees,B., Francklyn,C.S., Ehresmann,C. and Moras,D. (2000) Transfer RNA-mediated editing in threonyl-tRNA synthetase. The class II solution to the double discrimination problem. *Cell*, **103**, 877–884.

9. Ruan,L.L., Zhou,X.L., Tan,M. and Wang,E.D. (2013) Human cytoplasmic ProX edits mischarged tRNAPro with amino acid but not tRNA specificity. *Biochem. J.*, **450**, 243–252.
10. Nangle,L.A., De Crecy Lagard,V., Doring,V. and Schimmel,P. (2002) Genetic code ambiguity. Cell viability related to the severity of editing defects in mutant tRNA synthetases. *J. Biol. Chem.*, **277**, 45729–45733.
11. Nangle,L.A., Motta,C.M. and Schimmel,P. (2006) Global effects of mistranslation from an editing defect in mammalian cells. *Chem. Biol.*, **13**, 1091–1100.
12. Zhou,X.L., Du,D.H., Tan,M., Lei,H.Y., Ruan,L.L., Eriani,G. and Wang,E.D. (2011) Role of tRNA amino acid-accepting end in aminoacylation and its quality control. *Nucleic Acids Res*, **39**, 8857–8868.
13. Lee,J.W., Beebe,K., Nangle,L.A., Jang,J., Longo-Guess,C.M., Cook,S.A., Davisson,M.T., Sundberg,J.P., Schimmel,P. and Ackerman,S.L. (2006) Editing-defective tRNA synthetase causes protein misfolding and neurodegeneration. *Nature*, **443**, 50–55.
14. Fukunaga,R. and Yokoyama,S. (2005) Crystal structure of leucyl-tRNA synthetase from the archaeon *Pyrococcus horikoshii* reveals a novel editing domain orientation. *J. Mol. Biol.*, **346**, 57–71.
15. Zhou,X.L., Zhu,B. and Wang,E.D. (2008) The CP2 domain of leucyl-tRNA synthetase is crucial for amino acid activation and post-transfer editing. *J. Biol. Chem.*, **283**, 36608–36616.
16. Lincecum,T.L. Jr, Tukalo,M., Yaremchuk,A., Mursinna,R.S., Williams,A.M., Sproat,B.S., Van Den Eynde,W., Link,A., Van Calenbergh,S., Grotli,M. *et al.* (2003) Structural and mechanistic basis of pre- and posttransfer editing by leucyl-tRNA synthetase. *Mol. Cell*, **11**, 951–963.
17. Zhou,X.L., Wang,M., Tan,M., Huang,Q., Eriani,G. and Wang,E.D. (2010) Functional characterization of leucine-specific domain 1 from eukaryal and archaeal leucyl-tRNA synthetases. *Biochem. J.*, **429**, 505–513.
18. Yan,W., Tan,M., Eriani,G. and Wang,E.D. (2013) Leucine-specific domain modulates the aminoacylation and proofreading functional cycle of bacterial leucyl-tRNA synthetase. *Nucleic Acids Res*, **41**, 4988–4998.
19. Du,X. and Wang,E.D. (2003) Tertiary structure base pairs between D- and TpsiC-loops of *Escherichia coli* tRNA(Leu) play important roles in both aminoacylation and editing. *Nucleic Acids Res*, **31**, 2865–2872.
20. Hu,Q.H., Huang,Q. and Wang,E.D. (2013) Crucial role of the C-terminal domain of *Mycobacterium tuberculosis* leucyl-tRNA synthetase in aminoacylation and editing. *Nucleic Acids Res*, **41**, 1859–1872.
21. Palencia,A., Crépin,T., Vu,M.T., Lincecum,T.L., Martinis,S.A. and Cusack,S. (2012) Structural dynamics of the aminoacylation and proofreading functional cycle of bacterial leucyl-tRNA synthetase. *Nat. Struct. Mol. Biol.*, **19**, 677–684.
22. Yao,P., Zhu,B., Jaeger,S., Eriani,G. and Wang,E.D. (2008) Recognition of tRNALeu by *Aquifex aeolicus* leucyl-tRNA synthetase during the aminoacylation and editing steps. *Nucleic Acids Res*, **36**, 2728–2738.
23. Breitschopf,K., Achsel,T., Busch,K. and Gross,H.J. (1995) Identity elements of human tRNA(Leu): structural requirements for converting human tRNA(Ser) into a leucine acceptor in vitro. *Nucleic Acids Res*, **23**, 3633–3637.
24. Soma,A., Kumagai,R., Nishikawa,K. and Himeno,H. (1996) The anticodon loop is a major identity determinant of *Saccharomyces cerevisiae* tRNA(Leu). *J. Mol. Biol.*, **263**, 707–714.
25. Soma,A., Uchiyama,K., Sakamoto,T., Maeda,M. and Himeno,H. (1999) Unique recognition style of tRNALeu by *Haloferax volcanii* Leucyl-tRNA synthetase. *J. Mol. Biol.*, **293**, 1029–1038.
26. Fukunaga,R. and Yokoyama,S. (2005) Aminoacylation complex structures of leucyl-tRNA synthetase and tRNALeu reveal two modes of discriminator-base recognition. *Nat. Struct. Mol. Biol.*, **12**, 915–922.
27. Tindall,B.J., Ross,H.N.M. and Grant,W.D. (1984) Natronobacterium gen. nov. and Natronococcus gen. nov., Two New Genera of Haloalkaliphilic Archaebacteria. *Syst. Appl. Microbiol.*, **5**, 41–57.
28. Kamekura,M., Dyall-Smith,M.L., Upasani,V., Ventosa,A. and Kates,M. (1997) Diversity of alkaliphilic halobacteria: proposals for transfer of *Natronobacterium vacuolatum*, *Natronobacterium magadii*, and *Natronobacterium pharaonis* to *Halorubrum*, *Natrialba*, and *Natronomonas* gen. nov., respectively, as *Halorubrum vacuolatum* comb. nov., *Natrialba magadii* comb. nov., and *Natronomonas pharaonis* comb. nov., respectively. *Int. J. Syst. Bacteriol*, **47**, 853–857.
29. Li,Y., Wang,E. and Wang,Y. (1999) A modified procedure for fast purification of T7 RNA polymerase. *Protein Expr. Purif.*, **16**, 355–358.
30. Zhou,X.L., Fang,Z.P., Ruan,Z.R., Wang,M., Liu,R.J., Tan,M., Anella,F.M. and Wang,E.D. (2013) Aminoacylation and translational quality control strategy employed by leucyl-tRNA synthetase from a human pathogen with genetic code ambiguity. *Nucleic Acids Res*, **41**, 9825–9838.
31. Larkin,M.A., Blackshields,G., Brown,N.P., Chenna,R., McGettigan,P.A., McWilliam,H., Valentin,F., Wallace,I.M., Wilm,A., Lopez,R. *et al.* (2007) Clustal W and Clustal X version 2.0. *Bioinformatics*, **23**, 2947–2948.
32. Tamura,K., Peterson,D., Peterson,N., Stecher,G., Nei,M. and Kumar,S. (2011) MEGA5: molecular evolutionary genetics analysis using maximum likelihood, evolutionary distance, and maximum parsimony methods. *Mol. Biol. Evol.*, **28**, 2731–2739.
33. Gupta,R. (1984) *Halobacterium volcanii* tRNAs. Identification of 41 tRNAs covering all amino acids, and the sequences of 33 class I tRNAs. *J. Biol. Chem.*, **259**, 9461–9471.
34. Xu,M.G., Chen,J.F., Martin,F., Zhao,M.W., Eriani,G. and Wang,E.D. (2002) Leucyl-tRNA synthetase consisting of two subunits from hyperthermophilic bacteria *Aquifex aeolicus*. *J. Biol. Chem.*, **277**, 41590–41596.
35. Chen,X., Ma,J.J., Tan,M., Yao,P., Hu,Q.H., Eriani,G. and Wang,E.D. (2011) Modular pathways for editing non-cognate amino acids by human cytoplasmic leucyl-tRNA synthetase. *Nucleic Acids Res*, **39**, 235–247.
36. Wang,M., Zhou,X.L., Liu,R.J., Fang,Z.P., Zhou,M., Eriani,G. and Wang,E.D. (2013) Multilevel functional and structural defects induced by two pathogenic mitochondrial tRNA mutations. *Biochem. J*, **453**, 455–465.
37. Chan,P.P. and Lowe,T.M. (2009) GtRNAdb: a database of transfer RNA genes detected in genomic sequence. *Nucleic Acids Res*, **37**, D93–D97.
38. Hou,S., Larsen,R.W., Boudko,D., Riley,C.W., Karatan,E., Zimmer,M., Ordal,G.W. and Alam,M. (2000) Myoglobin-like aerotaxis transducers in Archaea and Bacteria. *Nature*, **403**, 540–544.
39. Fukuchi,S., Yoshimune,K., Wakayama,M., Moriguchi,M. and Nishikawa,K. (2003) Unique amino acid composition of proteins in halophilic bacteria. *J. Mol. Biol.*, **327**, 347–357.
40. Ortega,G., Lain,A., Tadeo,X., Lopez-Mendez,B., Castano,D. and Millet,O. (2011) Halophilic enzyme activation induced by salts. *Sci. Rep.*, **1**, 6.
41. Ito,S., Kobayashi,T., Ara,K., Ozaki,K., Kawai,S. and Hatada,Y. (1998) Alkaline detergent enzymes from alkaliphiles: enzymatic properties, genetics, and structures. *Extremophiles*, **2**, 185–190.
42. De Castro,R.E., Ruiz,D.M., Gimenez,M.I., Silveyra,M.X., Paggi,R.A. and Maupin-Furlow,J.A. (2008) Gene cloning and heterologous synthesis of a haloalkaliphilic extracellular protease of *Natrialba magadii* (Nep). *Extremophiles*, **12**, 677–687.
43. Krulwich,T.A. (1995) Alkaliphiles: 'basic' molecular problems of pH tolerance and bioenergetics. *Mol. Microbiol.*, **15**, 403–410.
44. Kitada,M., Kosono,S. and Kudo,T. (2000) The Na+/H+ antiporter of alkaliphilic *Bacillus* sp. *Extremophiles*, **4**, 253–258.
45. Aono,R., Ito,M. and Machida,T. (1999) Contribution of the cell wall component teichuronopeptide to pH homeostasis and alkaliphily in the alkaliphile *Bacillus lentus* C-125. *J. Bacteriol.*, **181**, 6600–6606.
46. Siddaramappa,S., Challacombe,J.F., Decastro,R.E., Pfeiffer,F., Sastre,D.E., Gimenez,M.I., Paggi,R.A., Detter,J.C., Davenport,K.W., Goodwin,L.A. *et al.* (2012) A comparative genomics perspective on the genetic content of the alkaliphilic haloarchaeon *Natrialba magadii* ATCC 43099T. *BMC Genomics*, **13**, 165.
47. Liu,H., Wu,Z., Li,M., Zhang,F., Zheng,H., Han,J., Liu,J., Zhou,J., Wang,S. and Xiang,H. (2011) Complete genome sequence of *Haloarcula hispanica*, a Model Haloarchaeon for

studying genetics, metabolism, and virus-host interaction. *J. Bacteriol.*, **193**, 6086–6087.
48. Cusack,S., Yaremchuk,A. and Tukalo,M. (2000) The 2 Å crystal structure of leucyl-tRNA synthetase and its complex with a leucyl-adenylate analogue. *EMBO J*, **19**, 2351–2361.
49. Landro,J.A. and Schimmel,P. (1993) Metal-binding site in a class I tRNA synthetase localized to a cysteine cluster inserted into nucleotide-binding fold. *Proc. Natl Acad. Sci. USA*, **90**, 2261–2265.
50. Landro,J.A. and Schimmel,P. (1994) Zinc-dependent cell growth conferred by mutant tRNA synthetase. *J. Biol. Chem.*, **269**, 20217–20220.
51. Zhu,B., Yao,P., Tan,M., Eriani,G. and Wang,E.D. (2009) tRNA-independent pretransfer editing by class I leucyl-tRNA synthetase. *J. Biol. Chem.*, **284**, 3418–3424.
52. Zhou,X.L., Tan,M., Wang,M., Chen,X. and Wang,E.D. (2010) Post-transfer editing by a eukaryotic leucyl-tRNA synthetase resistant to the broad-spectrum drug AN2690. *Biochem. J.*, **430**, 325–333.
53. Zhou,X.L., Ruan,Z.R., Huang,Q., Tan,M. and Wang,E.D. (2013) Translational fidelity maintenance preventing Ser mis-incorporation at Thr codon in protein from eukaryote. *Nucleic Acids Res*, **41**, 302–314.
54. Tan,M., Yan,W., Liu,R.J., Wang,M., Chen,X., Zhou,X.L. and Wang,E.D. (2012) A naturally occurring nonapeptide functionally compensates the CP1 domain of leucyl-tRNA synthetase to modulate aminoacylation activity. *Biochem. J.*, **443**, 477–484.
55. Li,L., Palencia,A., Lukk,T., Li,Z., Luthey-Schulten,Z.A., Cusack,S., Martinis,S.A. and Boniecki,M.T. (2013) Leucyl-tRNA synthetase editing domain functions as a molecular rheostat to control codon ambiguity in Mycoplasma pathogens. *Proc. Natl Acad. Sci. USA*, **110**, 3817–3822.
56. Lue,S.W. and Kelley,S.O. (2005) An aminoacyl-tRNA synthetase with a defunct editing site. *Biochemistry*, **44**, 3010–3016.
57. Zheng,Y.G., Wei,H., Ling,C., Xu,M.G. and Wang,E.D. (2006) Two forms of human cytoplasmic arginyl-tRNA synthetase produced from two translation initiations by a single mRNA. *Biochemistry*, **45**, 1338–1344.
58. Sivaram,P. and Deutscher,M.P. (1990) Existence of two forms of rat liver arginyl-tRNA synthetase suggests channeling of aminoacyl-tRNA for protein synthesis. *Proc. Natl Acad. Sci. USA*, **87**, 3665–3669.
59. Wu,Y.H., Chang,C.P., Chien,C.I., Tseng,Y.K. and Wang,C.C. (2013) An insertion peptide of yeast glycyl-tRNA synthetase facilitates both productive docking and catalysis of cognate tRNAs. *Mol. Cell Biol.*, **33**, 3515–3523.
60. Salazar,J.C., Ahel,I., Orellana,O., Tumbula-Hansen,D., Krieger,R., Daniels,L. and Söll,D. (2003) Coevolution of an aminoacyl-tRNA synthetase with its tRNA substrates. *Proc. Natl Acad. Sci. USA*, **100**, 13863–13868.
61. Reader,J.S., Ordoukhanian,P.T., Kim,J.G., de Crécy-Lagard,V., Hwang,I., Farrand,S. and Schimmel,P. (2005) Major Biocontrol of Plant Tumors Targets tRNA Synthetase. *Science*, **309**, 1533.
62. Roy,H., Zou,S.B., Bullwinkle,T.J., Wolfe,B.S., Gilreath,M.S., Forsyth,C.J., Navarre,W.W. and Ibba,M. (2011) The tRNA synthetase paralog PoxA modifies elongation factor-P with (R)-beta-lysine. *Nat. Chem. Biol.*, **7**, 667–669.
63. Guitart,T., Leon Bernardo,T., Sagales,J., Stratmann,T., Bernues,J. and Ribas de Pouplana,L. (2010) New aminoacyl-tRNA synthetase-like protein in insecta with an essential mitochondrial function. *J. Biol. Chem.*, **285**, 38157–38166.
64. Brown,J.R. and Doolittle,W.F. (1995) Root of the universal tree of life based on ancient aminoacyl-tRNA synthetase gene duplications. *Proc. Natl Acad. Sci. USA*, **92**, 2441–2445.
65. Andam,C.P., Harlow,T.J., Papke,R.T. and Gogarten,J.P. (2012) Ancient origin of the divergent forms of leucyl-tRNA synthetases in Halobacteriales. *BMC Evol. Biol.*, **12**, 85.
66. Fukunaga,R. and Yokoyama,S. (2007) The C-terminal domain of the archaeal leucyl-tRNA synthetase prevents misediting of isoleucyl-tRNA(Ile). *Biochemistry*, **46**, 4985–4996.